Arabian Journal of Chemistry (2020) 13, 7459–7481

King Saud University

Arabian Journal of Chemistry

www.ksu.edu.sa
www.sciencedirect.com

ORIGINAL ARTICLE

Efficiency of *Acacia Gummifera* powder as biosorbent for simultaneous decontamination of water polluted with metals

Bassem Jamoussi [a], **Radhouane Chakroun** [a,*], **Cherif Jablaoui** [b], **Larbi Rhazi** [b]

[a] *Department of Environmental Sciences, Faculty of Meteorology, Environment and Arid Land Agriculture, King Abdulaziz University, Jeddah, Saudi Arabia*
[b] *Institut Polytechnique UniLaSalle, Department Transformations &Agro-Ressources Unit, Beauvais, France*

Received 4 June 2020; accepted 22 August 2020
Available online 29 August 2020

KEYWORDS

Acacia Gummifera;
Adsorption;
Cadmium;
Lead;
Water treatment

Abstract Biosorbent materials represent an interesting alternative to classic methods of metal removal from industrial effluents. Acacia biomass showed a higher absorption capacity for heavy metals than living biomass. This study aimed to evaluate the bioadsorption of Lead and Cadmium onto *Acacia Gummifera* gum, using batch experiment. The structural characterization of the biosorbent was carried out using FT-IR, SEM, BET, TGA and DSC analysis. The adsorption equilibrium was reached within 15 min. A maximum uptake of 18.3 $mg.g^{-1}$ Pb^{2+} and 9.57 $mg.g^{-1}$ Cd^{2+} was achieved at pH 6.5. The metal ions seemed to be removed exclusively by ion exchange, physical sorption and chelation. The biomass of *A. Gummifera* powder was found to be effective for lead and cadmium removal with respectively 97% and 86% sorption efficiency at a concentration of 100 mg/L, in aqueous media. Parameters affecting adsorption capacities such as biosorbent dosage, initial metal concentration, temperature, and pH are discussed in detail. Furthermore, adsorption thermodynamics, kinetics, and equilibrium were studied and fitted by different models. Langmuir, Freundlich, Temkin and Dubinin–Radushkevich isotherms were used to compare adsorption data at equilibrium. The adsorption kinetics data were found to be best fitted by the pseudo-second-order model, and the adsorption isotherm was well fitted with the Langmuir model. The calculated thermodynamic parameters (ΔG^0, ΔS^0 and ΔH^0) indicated a spontaneous and exothermic biosorption of both metal ions onto *Acacia Gummifera*. Moreover, chromatograms obtained by size exclusion chromatography coupled with multi-angle laser light scattering detection system (SECMALLS) showed the formation of complexes between the arabinogalactan-peptide (AGP)

* Corresponding author at: Department of Environmental Sciences, Faculty of Meteorology, Environment and Arid Land Agriculture, King Abdulaziz University, P.O. Box: 80200, Zip Code: 21589, Jeddah, Saudi Arabia.
E-mail addresses: bissuomaj@kau.edu.sa (B. Jamoussi), rshagroon@kau.edu.sa (R. Chakroun), cherif.jablaoui@unilasalle.fr (C. Jablaoui), larbi.rhazi@unilasalle.fr (L. Rhazi).
Peer review under responsibility of King Saud University.

Production and hosting by Elsevier

https://doi.org/10.1016/j.arabjc.2020.08.022
1878-5352 © 2020 The Author(s). Published by Elsevier B.V. on behalf of King Saud University.
This is an open access article under the CC BY-NC-ND license (http://creativecommons.org/licenses/by-nc-nd/4.0/).

and glycoprotein (GP) Acacia moieties and the two studied metal ions. The analysis of the FTIR spectra of dried Acacia and that of Acacia loaded with lead and cadmium in aqueous media suggests that the surface functional groups such as amides and carboxy groups might be involved in the metal removal process.

The extent of adsorption for both metals increased along with an increase of the *A. Gummifera* biomass dosage. *A. Gummifera* biomass, which is safe, of low-cost, and highly selective, seems therefore to be a promising substrate for simultaneous trapping of Pd and Cd ions in aqueous solutions.

© 2020 The Author(s). Published by Elsevier B.V. on behalf of King Saud University. This is an open access article under the CC BY-NC-ND license (http://creativecommons.org/licenses/by-nc-nd/4.0/).

1. Introduction

Metal pollution is one of the major risks in today's world that lead to health hazards (Duruibe et al., 2007). Heavy metals pollution in seawater is a growing concern due to the increasing consumption of seawater by cooling facilities in coastal areas, and the production of fresh water to overcome the lack of water resources. Indeed, these trace elements are concentrated in water and aquatic microorganisms causing their bioaccumulation in aquatic resources. Heavy metals accumulated in these organisms can be transferred to humans through the food chain which may constitute a threat to human health (Kamran et al., 2013).

Lead and cadmium are among the elements having significant environmental health threats to humans. These elements cause toxic effects mainly by binding to, or interfering with organic sulfur compounds or groups in the body. Indeed, Lead has been reported to bind covalently to sulfhydryl groups, through binding to thiols groups of oxidized (GSSG) or reduced glutathione (GSH). These bindings disturb the GSSG/GSH balance which makes cells more prone to oxidative damage (Ahamed and Siddiqui, 2007). Lead has also been reported to be bioaccumulative and persistent in the environment. The effects of lead poisoning include serious damage to kidneys, liver, nervous system, and reproductive system. Moreover, severe Lead exposure has been associated with reprotoxic effects including decreased fertility, miscarriage, and developmental problems (Wani et al., 2015). Furthermore, Lanphear et al. (2005) reported an inverse relationship between Lead blood concentrations and intellectual quotient in children exposed to low environmental Lead levels.

Cadmium human toxicity assessment studies showed that this element may cause bone degradation, renal dysfunction, liver damage, hypertension, blood damage, and cancer (Bernard, 2008). Recent studies have shown that there is a relationship between chronic exposure to lead and cadmium, blood pressure values and the incidence of hypertension (Poreba et al., 2010).

Many processes have been investigated intensively during past years to remove heavy metals and organic pollutants from seawater and wastewater such as: chemical precipitation, coagulation/flocculation, reverse osmosis, nanofiltration membranes (Yang et al., 2018), complexation with a functionalized ligand anchored onto porous materials (Awual et al., 2019; Awuala, 2019), evaporation/distillation, ion exchange, coprecipitation/adsorption, ultrafiltration, biosorption etc. (Kurniawan et al., 2006).

However, these methods have drawbacks such as the excessive use of reagents, high cost, generation of toxic sludge and the use of energy consuming processes. Therefore, the investigation of new methods of heavy metals from water is still very important. The sorption process being very simple, economic, efficient and versatile has become a method of choice to remove toxic contaminants from wastewater (Lakherwal, 2014). The benefits of this decontamination method include low investment cost, simplicity of design and operation, and great performance compared to traditional systems. Recent studies have shown that biological materials derived from agricultural and agro-processing industry waste can have the ability to remove heavy metals by metabolic or physico-chemical mediated adsorption routes (Zabochnicka-Świątek and Krzywonos, 2014), and have sufficient ability to bind to metals with a certain selectivity (Kuyucak and Volesky, 1988).

Several researchers expected that this interesting perspective offers an economical alternative to remove toxic heavy metals from polluted waters with sufficiently high metal-binding capacity and facilitate the rehabilitation of the environment. Given the number of heavy metals and different biosorbent materials of different physico-chemical compositions, and in the absence of a generalized theoretical support, experimental tests of these effects still require a large volume of laboratory work in order to understand the absorption mechanisms for these metals. Several researchers have attempted to investigate different properties of biomass. Wang and Hung (2003) found that carbonized Acacia could be used for electromagnetic shielding. However, the main research application of these materials is their use as potential natural biosorbents for heavy metals. It has been reported (Eze et al., 2013) that heavy metals are adsorbed on the finest size particles.

Some studies have attempted to assess in detail the types of adsorption of heavy metals on different biological materials. These materials include sawdust, rice straw, soybean hulls and sugarcane bagasse. Exploration of these studied biomaterials has revealed that wood removes effectively heavy metals from aqueous solutions. Su et al. (2012) established the affinity order of sorption of metals on wood as follows: $Pb^{2+} \gg Cu^{2+} \gg Fe^{2+} > Cd^{2+} > Zn^{2+} > Ni^{2+} \geq Mn^{2+}$.

In a previous study, we showed that powder of Acacia may be considered as a promising biosorbent for the removal of traces of heavy metals such as Cd^{2+} and Pb^{2+} in wastewater (Bouazizi et al., 2016). Baig et al., (2010) have demonstrated the potential of the stem of *Acacia Nilotica* to remove Arsenic ions from different types of surface water samples. Manawi et al. (2018) used Acacia as a chelating agent followed by simple membrane filtration to remove lead (Pb^{2+}) from water.

Acacia gum contains in its composition glycoprotein type biopolymers. These glycoproteins include mainly Arabinogalactan-proteins (AGPs), arabinogalactan-peptide,

arabinogalactan-peptide, and highly glycosylated hydroxyproline-rich glycoprotein (Tan et al., 2012; Lamport and Várnai, 2013). Arabinogalactan-proteins (AGPs) are the main components of Acacia. The chemical structure of Acacia contains therefore, amino acids and different functional groups including amides and carboxy groups.

These groups confer to Acacia the amphiphilic character because its chemical structure includes hydrophilic polysaccharide fragments and hydrophobic protein chains (Mejia Tamayo et al., 2018). The study of Manawi et al. (2018) hypothesized that lead induces the formation of complexes by bridging the terminal carboxylate of glucuronic acid and Serine amino acid in Acacia macromolecules. Moreover, Khosa et al. (2014) suggested that the formation of Metal-Serine complexes was due to the interaction between the negatively charged surface and the metal which exhibits a deficiency in valence electrons. Several researchers have studied the stability of complexes between amino acids and metals (Smith et al., 1985; Lindholm-Lehto, 2019). The determination of stability constants of amino acid–metal complexes indicated that the strength of amino acids affinity with Pb^{2+} and Cd^{2+} was as follows: Glycine–Cd > Glycine–Pb > Alanine–Cd > Alanine–Pb > Histidine–Cd ~ Histidine–Pb > Threonine–Cd > Threonine–Pb > Phenylalanine–Cd ~ Phenylalanine–Pb ~ Aspartic acid–Cd ~ Aspartic acid–Pb ~ Methionine–Cd ~ Methionine–Pb ~ Glutamic acid–Cd ~ Glutamic acid–Pb > Serine–Cd ~ Serine–Pb (Khosa et al., 2014). However, although heavy metals coexist in wastewater, only few studies have been conducted on their competitive adsorption on Acacia. The excellent chelating property and ionic character of acacia involving the three major fractions (AGP, AG and GP) confers to the biosorbent a large capacity to bind metals with reduced time to reach equilibrium and low disposal cost. Therefore, we assume that acacia could be considered as one of the promising naturally abundant renewable biomaterials, requiring relatively low capital investment and low operational cost. Furthermore, the easy control of physico-chemical parameters should make the Acacia suitable for the decontamination of industrial effluents contaminated with toxic metals.

The typical interaction mechanisms between pollutants and *Acacia Gummifera* could be a combination of physical adsorption, ion-exchange, electrostatic interaction, complexation and H-bonding.

In this work, we studied the potential of biosorption of Acacia for the simultaneous removal of Lead and Cadmium from contaminated water. The influence of diverse parameters on heavy metals adsorption such as initial heavy metals concentration, temperature, biosorption kinetics, initial pH and sorption time was investigated. Equilibrium data were investigated using Langmuir and Freundlich isotherms models. Furthermore, thermodynamic parameters for the biosorption process such as ΔH^0, ΔS^0 and ΔG^0 have been also studied. Finally, the biosorbent used in this study has been compared with other similar biosorbents reported in the literature.

2. Materials and methods

2.1. Preparation of the biosorbent

Samples of *Acacia Gummifera* collected from the region of Tanent-Beni-Mellal (Morocco) were used as biosorbent for the simultaneous biosorption of Pb^{2+} and Cd^{2+} ions. The biosorbent samples were thoroughly washed with deionized water to remove extraneous matter and salts. Then, the samples were dried in an oven at 343 K for 24 h. The dried biomass was subsequently sieved in an electric sieve shaker with vertical vibration to obtain particles having an average size ranging from 150 to 500 μm. To remove the fine particles, the ground and sieved samples were subjected to successive washings with deionized water and then dried in an electric vacuum oven. The biosorbent material was then stored in hermetic containers until used in the tests. During the drying process, the removal of moisture, gas, and other possibly volatile chemicals led to the formation of cavities inside the acacia surface while preventing oxidation reactions and preserving the major characteristics of their constituents. The synthesis process and the adsorption mechanism (hydrogen bonding, electrostatic interactions and diffusion) are shown respectively in Fig. 1(a) and (b).

2.2. Reagents and equipment

All chemicals used in this study, were of Fluka or Aldrich analytical reagent grade or suprapur grade. Water purified with Milli-Q Integral water purification system (18.2 $M\Omega cm^{-1}$ conductivity) was used for dilutions. pH values in the aqueous phase were determined using a WTW 538 pH/temperature meter model. The Pb^{2+} and Cd^{2+} ions concentrations were determined in a single analytical run using Agilent 5110 Vertical Dual View (VDV) ICP-OES. FT-IR spectra of dried *Acacia Gummifera* sample were obtained with a BRUKER spectrometer model, using the KBR pellet method. The surface area, pore volume and pore diameter of *Acacia Gummifera* were determined based on the Brauner, Emmet and Teller (BET) method. Samples are dried using a Vacuum oven (Thermo Scientific Vacutherm Vacuum). SEM images were obtained using a JEOL electron microscope. The thermal behavior of the *Acacia Gummifera* during curing was followed up using thermogravimetric analysis. 10 mg sample was placed in an alumina crucible and heated at programmed temperature by rates of 10 °C/min in air environment. Thermal analysis was done using a Setaram thermal analyzer (SETARAM).

Size exclusion chromatography fractionation was performed using SEC-HPLC coupled with high Multi-Angle laser light scattering detection (SECMALLS) system consisting of an Eclipse3 F System (Wyatt Technology, Santa Barbara, CA, USA) serially connected to a UV detector (Agilent 1200, Agilent Technologies, Germany), a MALLS detector (Dawn multi-angle Heleos TM, Wyatt Technology Corporation, Europe) and an interferometric refractometer (RI) set at 35 °C (Optilab rEX, Wyatt Technology Corporation, Europe). The separation was performed using OHPAK SB 804HD and 806HD columns (Shodex, Tokyo, Japan) in series. The recorded MALLS, RI and UV data were processed using Astra software (v. 5.3.4.13, Wyatt Technology).

2.3. Preparation of aqueous solution of heavy metals

Standard solutions of Pb^{2+} ion and Cd^{2+} ion were prepared with de-ionized water in 1% HNO_3 from analytical grade of Lead(II) nitrate $Pb(NO_3)_2$ (1000 mg L^{-1}) and Cadmium(II) nitrate tetrahydrate ($Cd(NO_3)_2,4H_2O$) (1000 mg.L^{-1})

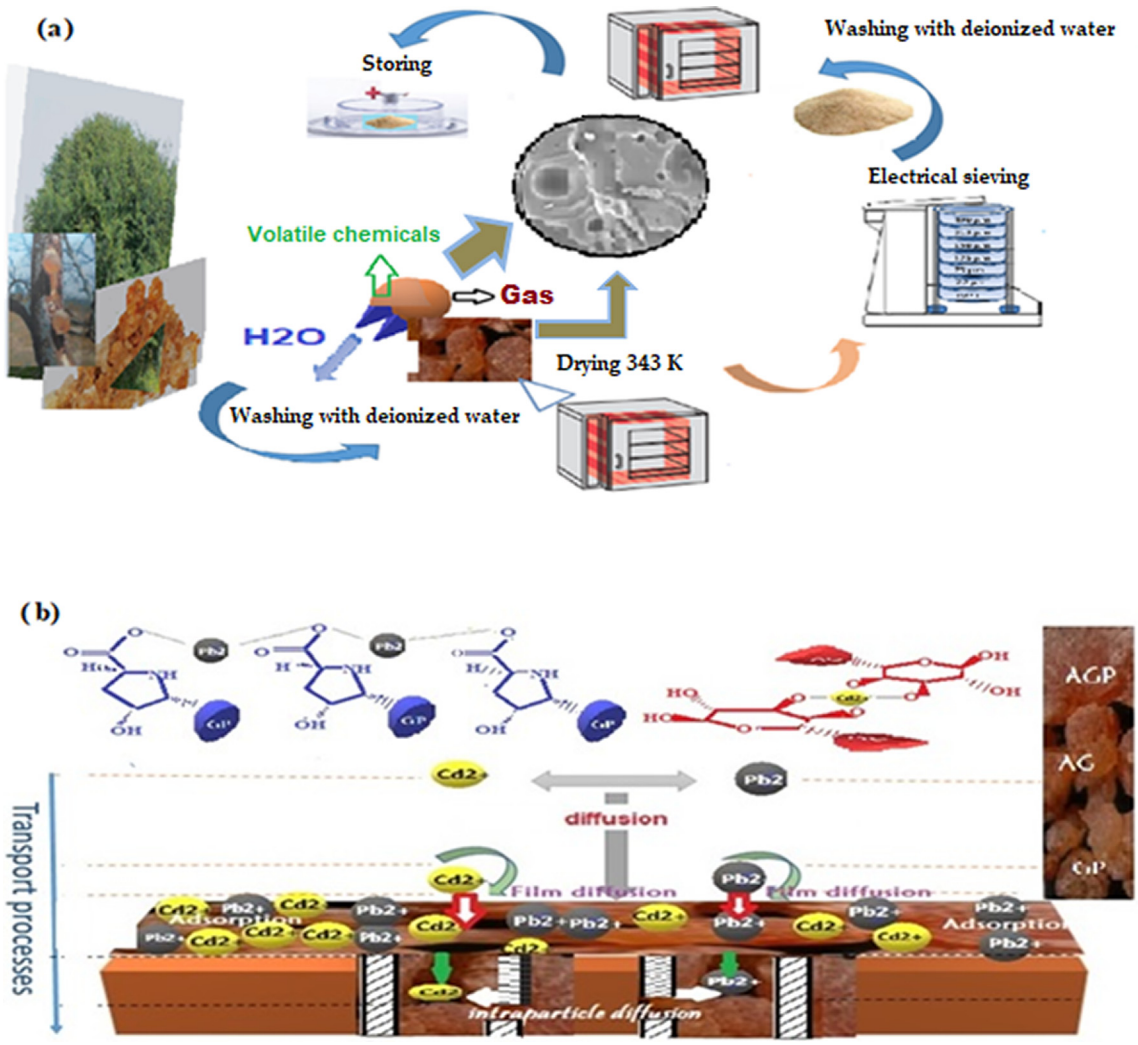

Fig. 1 Schematic representation of (a) the processing of the biosorbent and (b) the adsorption mechanism of Lead and Cadmium onto *Acacia Gummifera*.

(Sigma–Aldrich, 99%) by dissolving quantities of respective salts and were further diluted to the required experimental standard solutions. The desired pH of the solutions was obtained by adjusting the initial heavy metal solution either with an aliquot of 0.1 mol.L^{-1} NaOH or 0.1 mol.L^{-1} HNO_3 solution.

2.4. Biosorption studies of Cd^{2+} and Pb^{2+} ions on Acacia Gummifera

Biosorption experiments were carried out at the desired contact time, temperature, pH value and biomass dosage level using the batch method. In this method, a series of 125 mL glass Erlenmeyer flasks were filled with 50 mL metal ion solution at desired concentrations, then, the necessary amount of the biomass was added to each Erlenmeyer flask and agitated with a Heidolph MR 3000 magnetic stirrer at 350 rpm until equilibrium was attained. The obtained solutions were then centrifuged (Eppendorf Centrifuge 5410) and the supernatant liquids were subjected to the determination of Cd^{2+} and Pb^{2+} ions using inductively coupled plasma with optical emission spectroscopy (ICP-OES), after the filtration step using Whatman No. 42 filter paper. The experiments were repeated at 293,303 and 313 K using deionized water that was previously adjusted to pH6.5.

The amount of Cd^{2+} and Pb^{2+} adsorbed by *Acacia Gummifera* at equilibrium per unit mass of adsorbent qe (mg.g^{-1}) was calculated from the following equation:

$$q_e = \frac{(C_0 - C_e)V}{m} \tag{1}$$

where C_0 and C_e (in mg.L^{-1}) represent initial and equilibrium concentrations of both metal ions in aqueous solution, respectively. V (in L) is the volume of solution in liters (L) and m is the mass of the dry adsorbent in grams.

The removal efficiency R(p) of *Acacia Gummifera* was then estimated using mass balance equation (2):

$$R(p) = \frac{(C_0 - C_e)}{C_0} 100 \tag{2}$$

Biosorption experiments using 100 mg.L^{-1} metal ions solutions and a biomass dose of 0.8 g.L^{-1} were conducted for investigating the effect of pH. The contact time was varied from 0 to 150 min throughout the study, by taking samples at 10 min interval until 50 min, and every 50 min until 150 min.

2.5. Statistical analysis

Statistical analysis of data was conducted using computer software Microsoft Excel program. Simple linear regression was conducted in order to determine the slope and intercept of regression, with significant error $\alpha = 0.05$.

The linearization of the equations of adsorption isotherms implies a transformation of the data in a process that alters the structure of the errors, the normality of the least squares method and violates the assumptions of error variance. For this reason, the linear parameters obtained by the Freundlich model produce isotherms which correspond best to the data at low concentrations, while those of Langmuir tend to correspond better to the isothermal data at higher concentrations (Allen et al., 2004; Ayoob and Gupta, 2008). Consequently, it is essential to correctly choose the error function when assessing the fit of experimental data to the linearized isotherm model, as it may affect the derived parameters. For the aforementioned drawbacks of linear procedures, the sum of squares of errors (SSR) error function is widely used to decide which model provides the best fit. However, among the disadvantages of (SSR), is that when the concentration increases, the errors and therefore their squares increase.

In order to overcome the factual error, the hybrid fractional error function (HYBRD) (Allen et al., 2004; Anirudhan and Radhakrishnan, 2009; Foo and Hameed, 2010) was used in this work. HYBRD has been developed to improve SSR at low concentrations. In this approach, the SSR is divided by the measured value and the degree of freedom of the system is included. A similar approach using modification of the distribution of the mean errors, taking into account the number of degrees of freedom of the system was also adopted. The calculated standard deviation is expressed as a percentage of Marquardt (MPSD) (Allen et al., 2004; Anirudhan and Radhakrishnan, 2009; Foo and Hameed, 2010).

The sum of squares of the errors (SSR) $\sum_{i=1}^{N} (q_{i,exp} - q_{i,cal})^2$ (3)

Hybrid fractional error function (HYBRID) $\frac{100}{N-p} \sum_{i=1}^{N} \times \frac{(q_{i,exp} - q_{i,cal})^2}{q_{i,exp}}$ (4)

Marquardt's percent standard deviation (MPSD) $100 \times \sqrt{\frac{1}{N-p} \sum_{i=1}^{N} \frac{(q_{i,exp} - q_{i,cal})^2}{q_{i,exp}}}$ (5)

Where:

$q_{i,exp}$: Experimental data values
$q_{i,cal}$: Data values calculated from the model
N: Number of data
p: Number of model parameters

3. Results and discussion

3.1. Biosorbent characterization

3.1.1. Fourier transform infrared (FT-IR) analysis

Spectral analysis by FT-IR makes it possible to highlight the chemical functional groups of a dried gum *Acacia Gummifera* material. The FT-IR spectrum of the Acacia gum samples were acquired in the frequency range of 400–4000 cm^{-1} (Fig. 2).

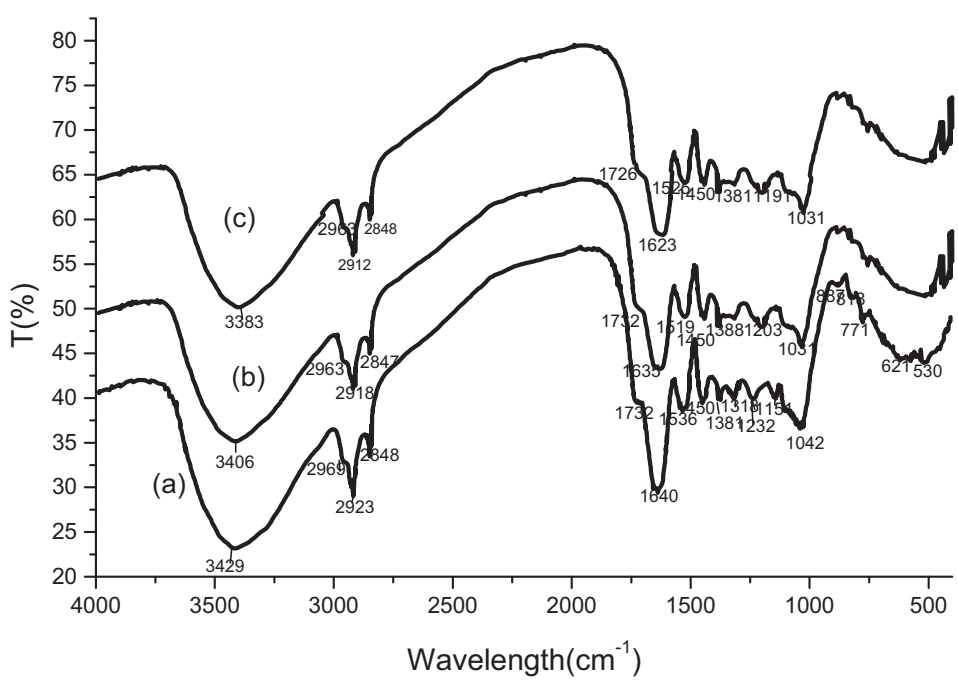

Fig. 2 FTIR spectra of *Acacia Gummifera* (a) before and after biosorption with Pb^{2+} ions (b) or Cd^{2+} ions (c).

The FTIR spectra of dried natural unloaded and heavy metals loaded Acacia gum were compared to obtain more information about potential interactions between metal ions and biomass functional groups (Fig. 2). We may note the presence of ether signals (C-O-C) in sugar units absorbed as strong intensities around 1161 and 1151 cm^{-1} (Kačuráková et al., 2000). Fig. 2(a) shows a strong wide band with higher intensity at 3429 cm^{-1} due to the overlapping of –OH stretching vibrations (Smith, 2017). Hydroxyl and carboxyl functional groups contained in Acacia molecular structure may interact with protons and metals. The comparison of stretching vibration frequency of OH groups shows that relative positions of wide bands of Pb and Cd have been slightly modified in the spectra of loaded biosorbent (Fig. 2b and 2c) compared to the main peak of non-loaded acacia (Fig. 2a), which shifted from 3429 to 3406 cm^{-1} in case of Pb^{2+} and to 3383 cm^{-1} in case of Cd^{2+}. These results suggest that chemical interactions occurred on the Acacia surface between metal ions and hydroxyl groups. The shift can be explained by chelation/adsorption of metal ions with functional groups such as carboxylate ($RCCO^{-}$) and hydroxyl (–OH) as reported by (Gedam and Dongre, 2015). Furthermore, the absorption bands of carboxyl groups at around 1640 cm^{-1} (asymmetrical COO– stretching vibration) is most marked in polysaccharides FT-IR spectrum (Nejatzadeh-Barandozi and Enferadi, 2012), which indicates high carboxyl group content of the studied Acacia gum. The feature bands of protein are all observed in *Acacia Gummifera* samples spectra. Main amides (I) peak's positions in loaded acacia spectra (Fig. 2b and 2c) shifted slightly (1646 cm^{-1} for Pb^{2+} and 1639 cm^{-1} for Cd^{2+}), and had their intensity decreased in comparison with raw Acacia (Fig. 2a). Besides, other FT-IR characterization studies reported around the wavenumber region 1370–1230 cm^{-1}, the contribution of proteins (Band amide III) (Barth and Zscherp, 2002), phenolic esters attached to polysaccharides (Sene et al., 1994), and methyl ester groups (CH_3-COO^{-}), included in the structure of 4-O-Methyl-glucuronic acid and proteins reported as components of acacia gums (Barth and Zscherp, 2002; Synytsya et al., 2003). In the present work, FTIR spectra analysis around this wavenumber region (1370–1230 cm^{-1}) is in agreement with a polysaccharide structure of Acacia gum reported by several scientists (Fig. 2 a,b,c). Furthermore, the characteristic spectral bands produced by polysaccharides' skeletal backbone and side chains stretching vibrations are noted in the wavenumber region between 1200 and 800 cm^{-1}. The main vibrations include ring vibrations overlapped with (C-OH) side groups and (C-O-C) glycosidic bond stretching vibrations (-Kačuráková et al., 2000). The absorption profile at this wavenumber region is indeed considered as a carbohydrate fingerprint. The peak 1042 cm^{-1} shifted to 1031 cm^{-1} after biosorption of metal ions indicating that (C-OH) side groups of polysaccharides may have been involved in the biosorption of Cd^{2+} and Pb^{2+} onto *Acacia Gummifera*.

Finally, no frequency change was observed at the wavenumber region 880–920 cm^{-1}, corresponding to β-glycosidic bonds involved in galactopyranose units linkages (Kačuráková et al., 2000).

3.1.2. SEC-HPLC analysis

Despite the importance of complexation reactions that may be involved in heavy metal adsorption, most of the experimental studies on adsorption at the solid/solution interface did not generally considered the effects of metal-binding ligands. In this part of the study, we aim to provide some details concerning the adsorption of lead and cadmium at the acacia /solution interface, and highlight the role of complexation in the adsorption process. The separation of the different fractions of *A. Gummifera* gum has been performed using Size Exclusion Chromatography coupled with high Multi-Angle Laser Light scattering (SECMALLS), UV and RI detection systems, according to the chromatographic method reported by Rhazi et al. (2020).

Fig. 3(a) shows a typical set of chromatograms of *Acacia Gummifera*. The chromatographic profile is consistent with chromatograms obtained by Rhazi et al. for Acacia Senegal gums. In this investigation, the elution recovery was 100%. For A. *Gummifera* gum samples, the RI profile showed two distinct peaks. The first small peak (elution 25–30 min) was attributed to the arabinogalactan-protein (AGP) with a – 8% protein content and molecular weight starting from 1400 kDa. The second large peak (elution 30–35 min) is the main population as it accounts for −87% was attributed to the arabinogalactan (AG) fraction displaying a molecular weight about 300 kDa. Finally, a much smaller population (~2%) consists of glycoprotein (GP) and displays the highest protein content (25–50%). The UV (214 nm) elution profiles which are mostly sensitive to the peptide bond were significantly different from the RI profiles, showing a huge peak with shoulder, covering the first two fractions mentioned earlier. Besides, the formation of complexes allows identifying the sequestering fraction of *A. Gummifera* for Cd^{2+} and Pb^{2+}. After solubilization of the Acacia sample, Cadmium and Lead solutions were added and subsequently separated by SEC–HPLC. Fig. 3 (b) and (c) show that AGPs, GP and GA were eluted from the SEC–HPLC column as metal-complexes with better peak's resolution, which confirms the fact that the AGPs, GP and GA acted as chelators and that they are excellent bidentate ligands to bind cadmium and lead ions in aqueous solution.

Fig. 3 (b) shows a better resolution of the chromatographic peaks with a decrease in the elution time. It is also observed that the AGP and GP fractions are more involved in the complexation of Pb^{2+} than AG fraction, resulting in sensitive UV detection of peptide bond. This confirms the selectivity of *Acacia Gummifera* towards heavy metals. This selectivity can be enhanced by anchoring synthesized ligand that showed high selectivity and removal yield (Awualb, 2019)

On the other hand, a slight shift of the elution time of the AG fraction. It is reasonable to assume that the complexation of lead could be attributed to the chelating property of AGP and GP.

Fig. 3 (c) clearly shows that the AG part has undergone a significant reduction in its chromatographic peak detected by IR, which is specific for polysaccharides. This suggests that the complexation occurs mainly at the AG fraction level.

The displacement of the overlapped chromatographic peaks observed in Fig. 3(b) and 3(c) could be due to the shift in the balance towards the formation of complexes in the presence of the metal ions.

Fig. 4 depicts a schematic representation of Lead and Cadmium complexation with some of the potential chelating groups of AGP and AG, respectively. The involved mechanisms include surface adsorption and complexation by ligands associated with the extracellular polymers of *Acacia Gummifera*.

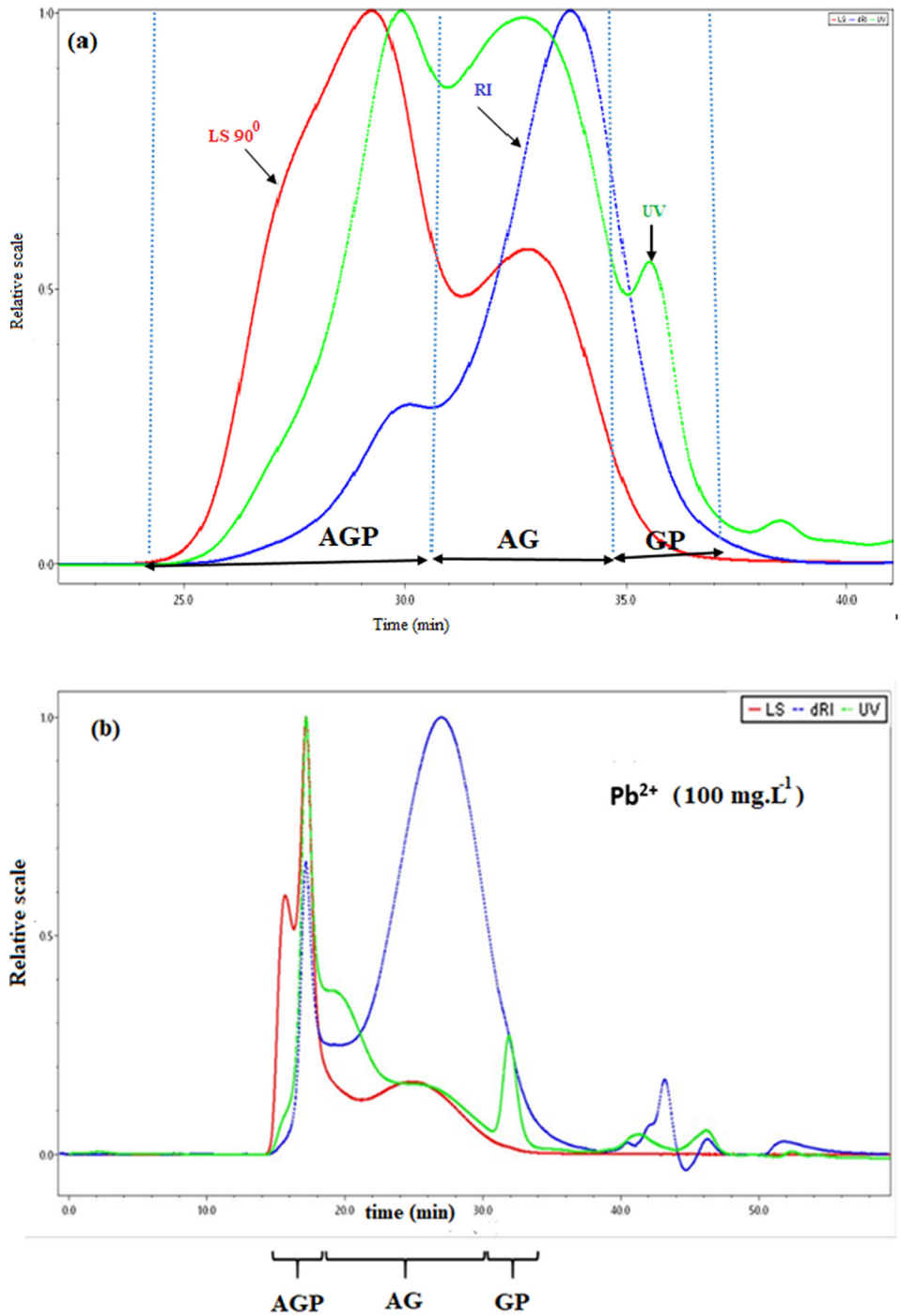

Fig. 3 *SEC-HPLC / UV*-MALLS-RI chromatogram of (a) *A. Gummifera* gum sample, (b) Lead complexation with some functional groups of AGP and GP fraction and (c) Cadmium complexation with some AG functional groups.

3.1.3. Characterization of biosoerbent surfaces by SEM

The purpose of the SEM analysis is to illustrate the porosity of a material which conditions the area of the specific surface and the number of active sites on which metal ions can be fixed. In order to study the porosity of *Acacia Gummifera*, SEM images of 3–100 μm Acacia particles were taken at different magnifications (100,500, 1000, 3000,6000, and 10,000 times) (Fig. 5). At 200 μm scale, we can note the presence of numerous macropores of different sizes and shapes (Fig. 5,f). These macropores have diameters in the range of 20–100 μm. Smaller size pores were also visible. Also, the surface of the pores is completely smooth and very similar to the external surface of the analyzed biopolymers. This morphology and texture are found in biomaterials highly glycosylated with arabinogalactan-peptide (-Kačuráková et al., 2000), which confirms our previous findings with the FTIR analysis. Fig. 5(c, d) obtained at a mag-

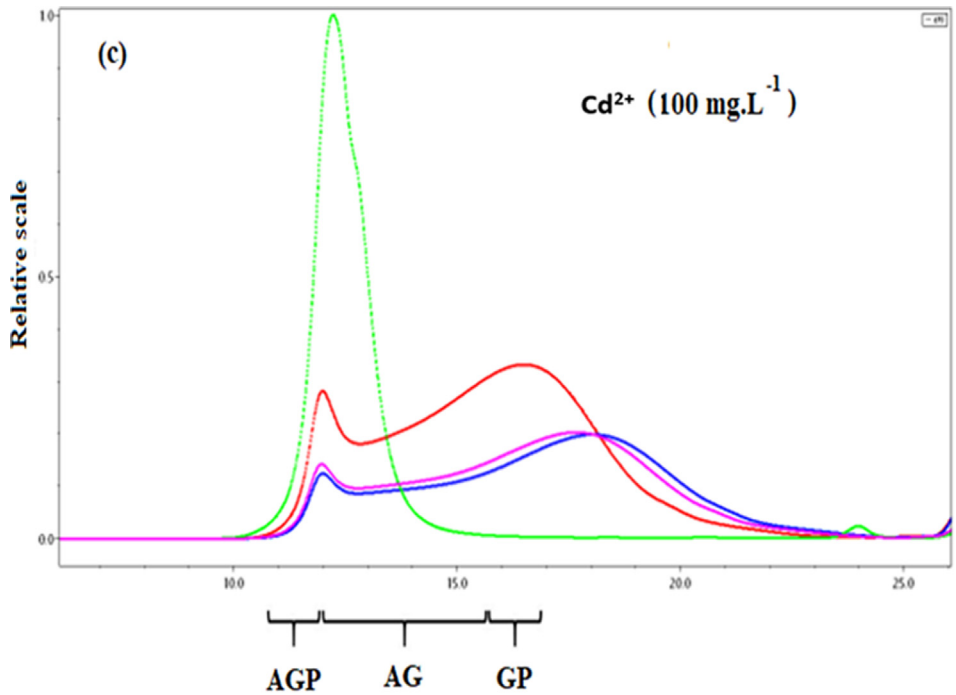

Fig. 3 (*continued*)

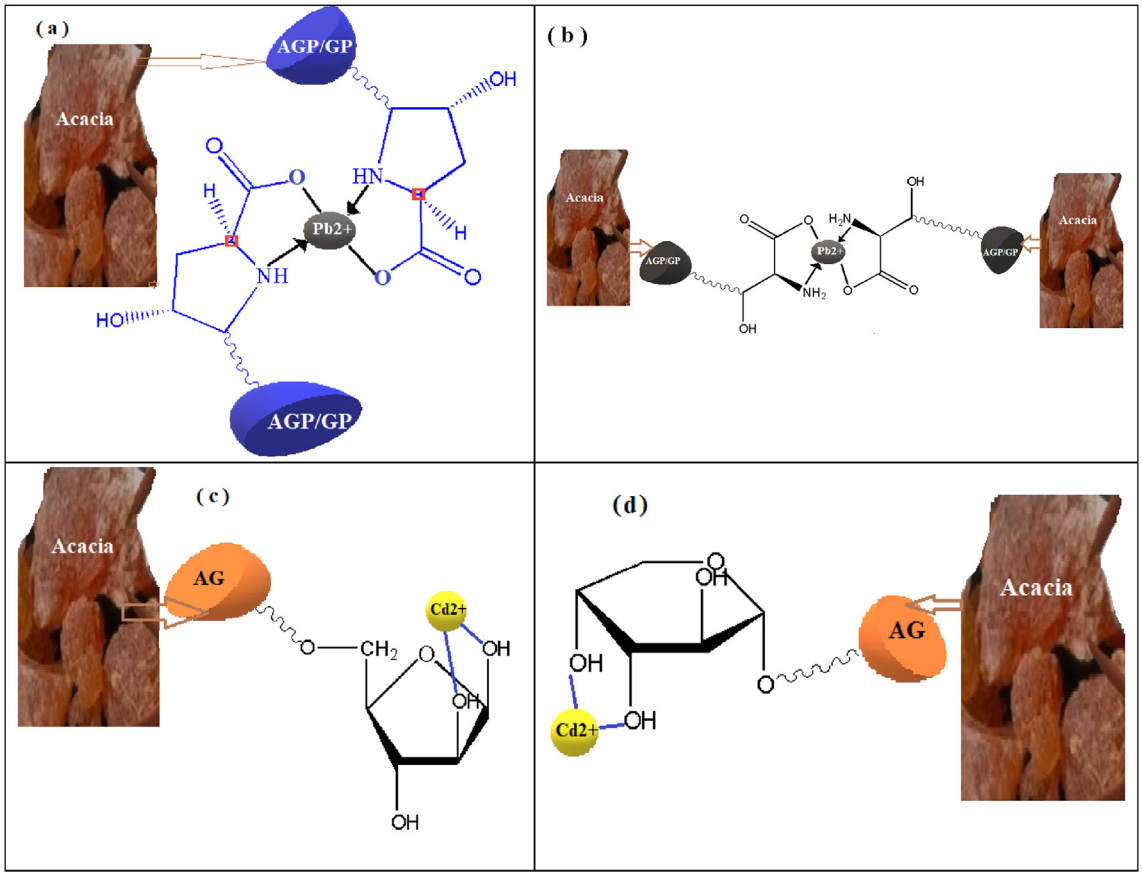

Fig. 4 Schematic diagram of complexation of Cd^{2+} and Pb^{2+} ions on the extracellular polymers of *Acacia Gummifera* (a) Lead complexation with hydroxyproline amino acids present in AGP and GP macromolecules, (b) Lead complexation with serine amino acids present in AGP and GP macromolecules, (c) Cadmium complexation with arabinopyranose in AG, (d) Cadmium complexation with arabinofuranose in AG macromolecules.

nification of 6000X and 10,000X respectively, are characterized by the presence of a hole similar to a hollow half sphere, having a radius around 11.25 μm. This means that this very porous architecture could enable Acacia particles to trap even hydrated Pb^{2+} and Cd^{2+} whose radii are 4.01 and 4.26A respectively, and therefore, are less than the radius of the hole observed on the surface of the biomaterial. Given these dimensions, it can be expected that Pb will be more readily adsorbed through the internal sorption surface than Cd.

As seen in the Fig. 5(f), the studied *Acacia Gummifera* powder has wide particle size distribution. Also, some large agglomerates were observed along with smaller particles. However, as shown in Fig. 6, the particle radius distribution showed higher distribution in the range of 25 to 70 μm. The estimated mean particle radius obtained from a normal distribution fitting (using STATGRAPHIC XVI centurion software) is − 46 μm.

3.1.4. Thermal analysis of Acacia Gummifera gum by TGA and DSC

The experiment of thermal degradation of acacia was conducted from 30 °C to 800 °C at the heating rate of 10 °C/min. The thermogram obtained by thermal degradation of Acacia by the thermogravimetric analysis (TGA) and the

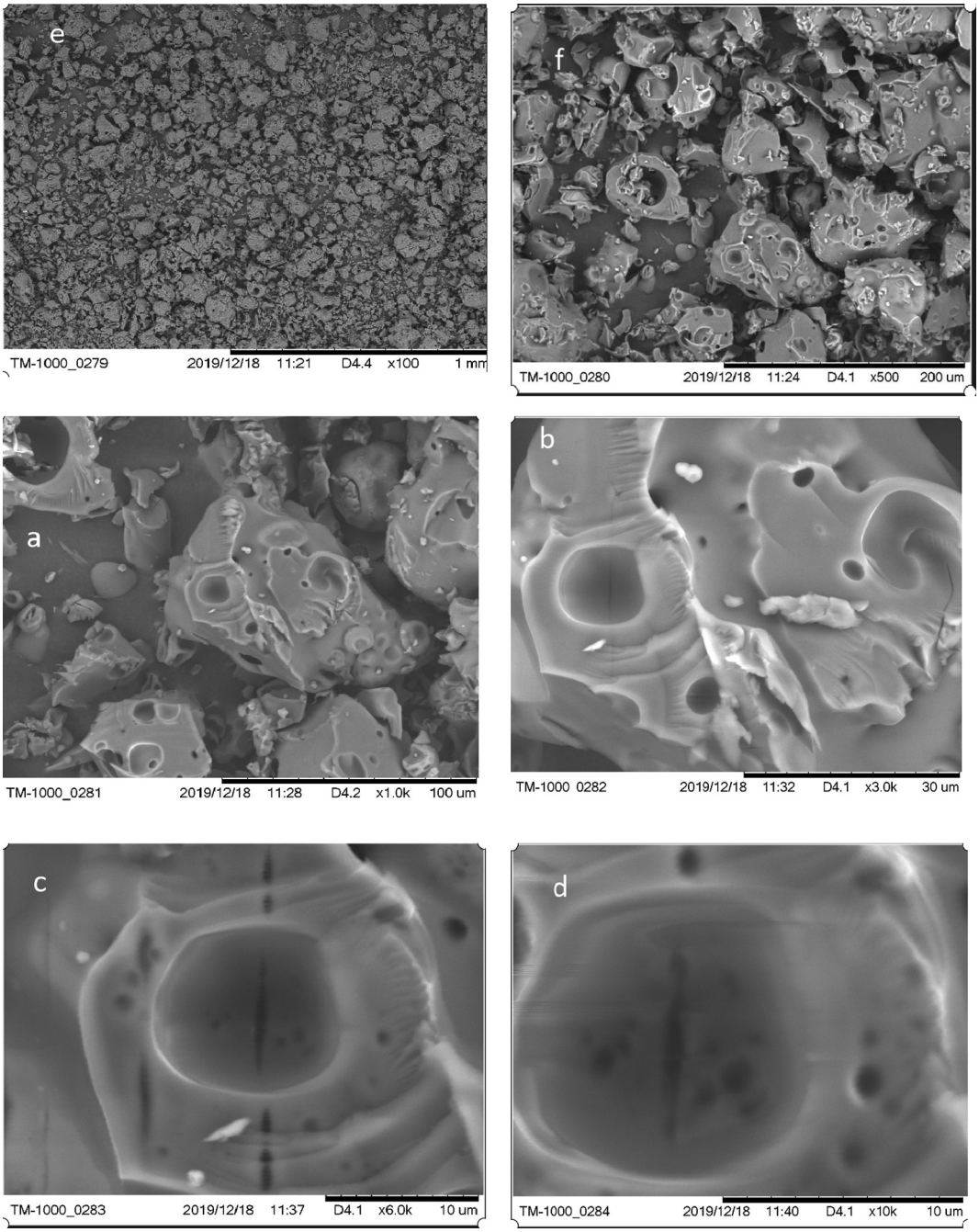

Fig. 5 Micrography of Acacia gum at 6 magnifications: a) 1000×, b) 3000×, c) 6000× and d) 10,000×, e) 100×, f) 500×.

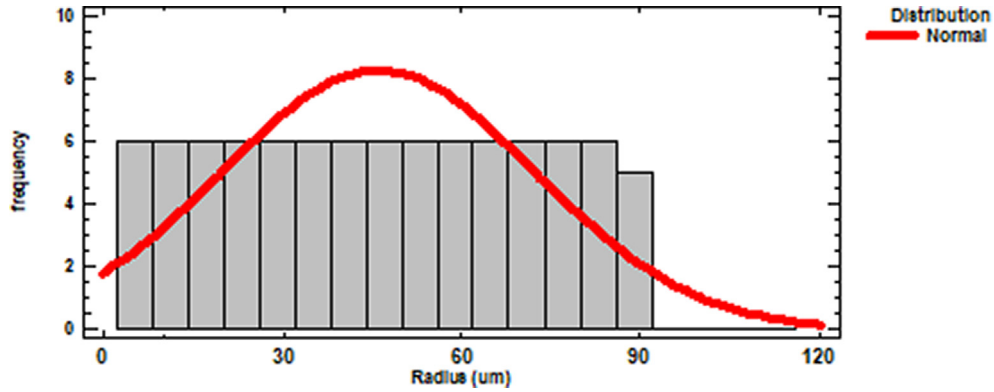

Fig. 6 *Acacia Gummifera* particle radius distribution.

differential scanning calorimetry (DSC) yielded to the results depicted in Fig. 7 and Fig. 8 respectively.

Thermogravimetric analysis revealed two endothermic peaks (Fig. 7), showing two stages of thermal degradation:

- In the first stage (30–120 °C), the 5% weight loss is in relation with water removal from biomass.
- The second peak reflects heat absorbed by polysaccharides during decomposition at 230–330 °C. The weight loss exceeds 53.74% and is due to the release of gaseous compounds CO_2, CH_4, CO, H_2. These results are consistent with the characteristic stretching vibration of the OH group observed at 3429 cm^{-1} (Fig. 2). Moreover, the release of gaseous compounds CO_2 and CO from biomaterial confirms the existence of C = O due to the thermal cleavage of CO_2 from the carbohydrate skeleton identified in the FT-IR spectrum (Fig. 2) at around 1640 cm^{-1} (asymmetrical COO– stretching vibration). The onset temperature at 288 °C indicated that Acacia gum was relatively stable under 200 °C, whereas decomposition occurred at about 280 °C (Chen et al., 2015).
- In the third temperature interval (400–600 °C), an exothermic peak is observed at around 425 °C, with a weight loss of 6.95%. This last stage would correspond to the carbonization zone.

3.1.5. Analysis results by BET

The specific surface area of the adsorbent gum *Acacia Gummifera* was determined using multipoint BET method. The obtained value was as high as 367.30 $m^2.g^{-1}$. This value appears to be in good agreement with the BET surface area reported by Baig et al. (Baig et al., 2010), characterized by an estimated specific surface of 350 m^2/g. Fig. 9 shows the Adsorption/desorption isotherm of *Acacia Gummifera* gum at 77 K.

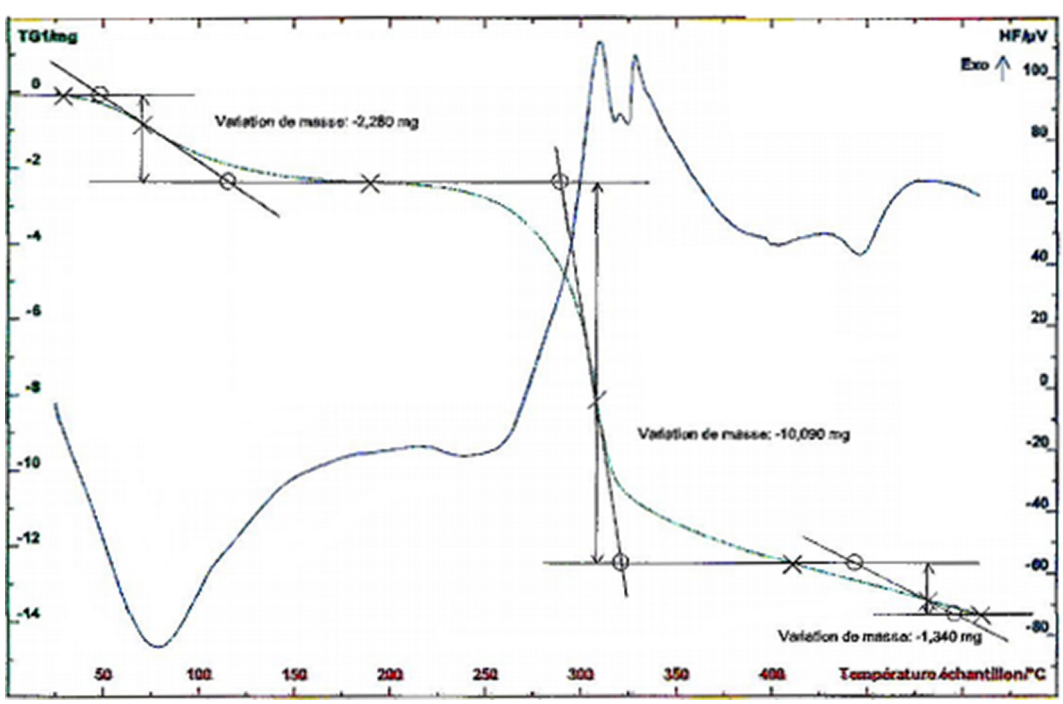

Fig. 7 TGA curves of Acacia gum.

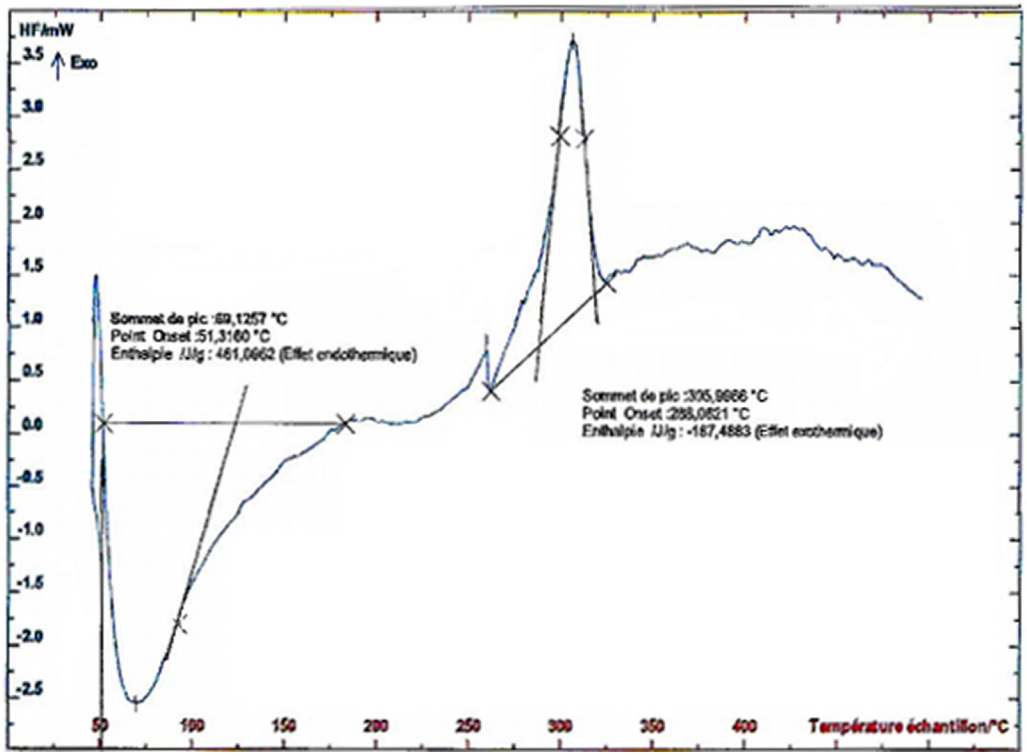

Fig. 8 DSC curves of acacia gum.

3.2. Effect of pH

It is well known that the pH of the solution is one of the most important factors for the removal of heavy metals from the aqueous solution. The effect of the pH of the solution could be explained by the modification of the surface charges of the biosorbent, and the degree of ionization of metal ions in an aqueous solution (Sharma and Bhattacharyya, 2005; Özer, 2007). The results of the adsorption capacity for different pH values are presented in Fig. 10.

It was observed from Fig. 10 that the biosorption capacity increases rapidly when the pH shifts from 5 to 6. Biosorption increases from 40% to 97% for lead, and from 32% to more than 89% for cadmium. At acidic pH < 4, metal ions exist as Pb^{2+} and Cd^{2+} and biosorbent surface is covered by H^{+} ions. Therefore, the affinity of metal ions with the surface of biosorbent is low. This weak adsorption could be explained by the presence of electrostatic repulsion between these positively charged species on the adsorption surface and metal ions. Furthermore, at low pH values (pH < 5, $pK_H \approx 5$) carboxylic groups are protonated (Vilar et al., 2007). This phenomenon has been observed by other authors (Galedar and Younesi, 2013; Amini Malihe et al., 2013). With a pH increase from 4 to 7, deprotonation occurs on the biosorbent surface, which particularly involves glucuronic acid and 4-O-methylglucuronic acid, promoting electrostatic attraction between the positively charged metal ions and the biosorbent

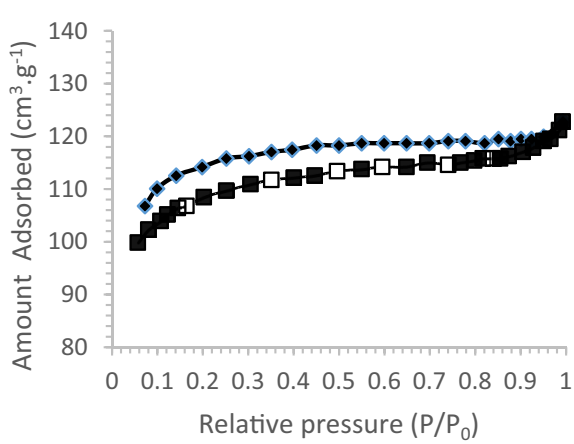

Fig. 9 Adsorption/desorption isotherm of *Acacia Gummifera* gum at 77 K.

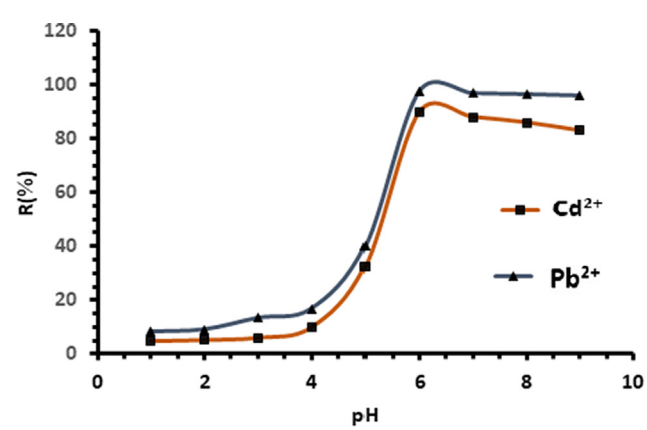

Fig. 10 Effect of pH on the percentage of biosorption of Cd^{2+} and Pb^{2+} ions onto *Acacia Gummifera* biomass.

surface negatively charged at this pH range, and consequently increasing the efficiency of adsorption. On the other hand, the contribution of carboxylic groups for binding Pb^{2+} and Cd^{2+} is important at the pH range (6–7) (pKH > 8.0), because the hydroxyl groups are not dissociated in this pH range (Vilar et al., 2007).

Similar results were reported by Munagapati et al. (2010) who studied the biosorption of Pb^{2+} and Cd^{2+} from aqueous solutions by fungus biomass. The optimal pH was found to be equal to 6.5. At pH > 6.5 a dissociation of metals from the surface may have occurred. This may be explained by the dissociation of surface hydroxyl groups from species of low solubility, including $Pb(OH)_4^{2-}$, $Pb(OH)_2$ and $[Pb(OH)]^-$ as well as $[Cd(OH)]^-$ and $Cd(OH)_2$. From Fig. 10, we may assume that adsorption can take place in the pH range of 5–9 according to two mechanisms: electrostatic adsorption of species such as $Cd(OH)^+$ and $Pb(OH)^+$, and precipitation of $Cd(OH)_2$ and Pb $(OH)_2$ metal ions species, which is in agreement with the results obtained by (Farooq et al., 2010). However, the optimal pH of metal ion complexation which allows the maximum removal of lead and cadmium simultaneously seems to be equal to 6.5. The mechanism of the ion exchange process has been confirmed by experimental results. During this process, the metal ions can move through the pores of *Acacia* and displace the exchangeable cations, particularly hydroxyl groups on the surface of the biosorbent.

3.3. Effect of biosorbent dosage

The effect of biosorbent dosages for Pb^{2+} and Cd^{2+} ions removal from aqueous solution was investigated at different adsorbent doses. Ten varying doses of biomass ranging from 0.20 to 2.0 g were selected and added to samples of 100 mg. L^{-1} metal ions solution at pH 6.5. The highest removal yield was obtained at biosorbent doses of about 0.8 g (Fig. 11).

As shown in Fig. 11, the maximum biosorption rate was obtained when using a biosorbent dose of 0.8 g.L^{-1}. At this dose, up to 97% Pb^{2+} and 86p Cd^{2+} were adsorbed onto *Acacia Gummifera* biomass. These findings are consistent with results reported in other studies (Farooq et al., 2010; Subbaiah et al., 2011). Therefore, the optimal biomass dosage was fixed at 0.8 g for further experiments.

3.4. Effect of the contact time

Metal aqueous solutions of Pb^{2+} and Cd^{2+} (at pH = 6.5) are brought into contact with 0.8 g of *Acacia Gummifera* biomass, during the interval time from 0 to 300 min. Fig. 12 (a, b) illustrates the biosorption of Pb^{2+} and Cd^{2+} at different concentrations on the biomass of *Acacia Gummifera*. The curves indicate that the biosorption occurs rapidly at the initial stage and then slowed down gradually slowed down as the equilibrium was reached.

The shape of the curves suggests a rapid saturation of the available surface active sites, especially for lead metal ion (which, compared to Cd ions, needs only few minutes to reach the maximum of biosorption capacity) (Fig. 13). This behaviour can be attributed to the effect of the competition between the two elements. A high biosorption capacity of *Acacia Gummifera* for Pb^{2+} has been observed, with an increase from 36% to 73% in the time interval between 10 and 15 min. Therefore,

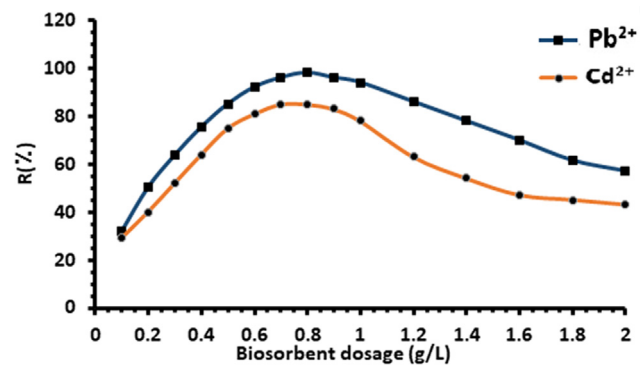

Fig. 11 Effect of biosorbent dosage on metal ions biosorption yield (%) onto *Acacia Gummifera* biomass. Experimental conditions: initial concentration of each metal ion for Pb^{2+} and Cd^{2+}: 100 mg.L^{-1}; contact time: 2 h, temperature 303 K, pH = 6.5.

it may be deduced that the selectivity order is $Pb^{2+} > Cd^{2+}$, corresponding to a biosorption efficacy of 97% and 86%, respectively.

3.5. Effect of initial metal concentration

One of the important parameters that affect the driving force of the biosorption process is the initial concentration (Pearson, 1963). As shown in Fig. 14, biosorption capacity of *Acacia Gummifera* biomass increases with increasing initial concentrations until saturation of surface sites.

It can be deduced from Fig. 14 that absorption rate exceeds 85% for both Pb^{2+} and Cd^{2+} at low concentration levels (< 100 mg/L), suggesting that there are enough available sorption sites. However, at a higher concentration level (> 150 mg / L) a decrease in the slope of the curve is observed, which means that the quantity of metal ion is greater than the available sorption sites.

3.6. Biosorption kinetics

In order to determine the stage which controls the speed of adsorption of Cd^{2+} and Pb^{2+} ions, the adsorption kinetics provides important information on the mechanism and on the modeling of the biosorption process. The Lagergren's pseudo-first-order and pseuso-second-order were used to study the biosorption of both metal ions, whereas the intra-particle diffusion model was used to determine the rate controlling step. Values obtained for these parameters, with initial concentrations varying from 20 to 100 mg L^{-1} are depicted in Table 1.

In the pseudo-first-order model (Soco and Kalembkiewicz, 2016), the adsorption rate of Cd^{2+} and Pb^{2+} ions onto *Acacia Gummifera* is proportional to (q_e-q_t) and can be expressed as follows:

$$\frac{dq}{dt} = k_1(q_e - q_t) \tag{6}$$

Where k_1 is the first-order rate constant (min^{-1}), q_t and q_e (mg. g^{-1}) are the amounts of the metal ions sorbed at equilibrium time t(min).

The integration of this equation results in a linear form of the pseudo-first-order

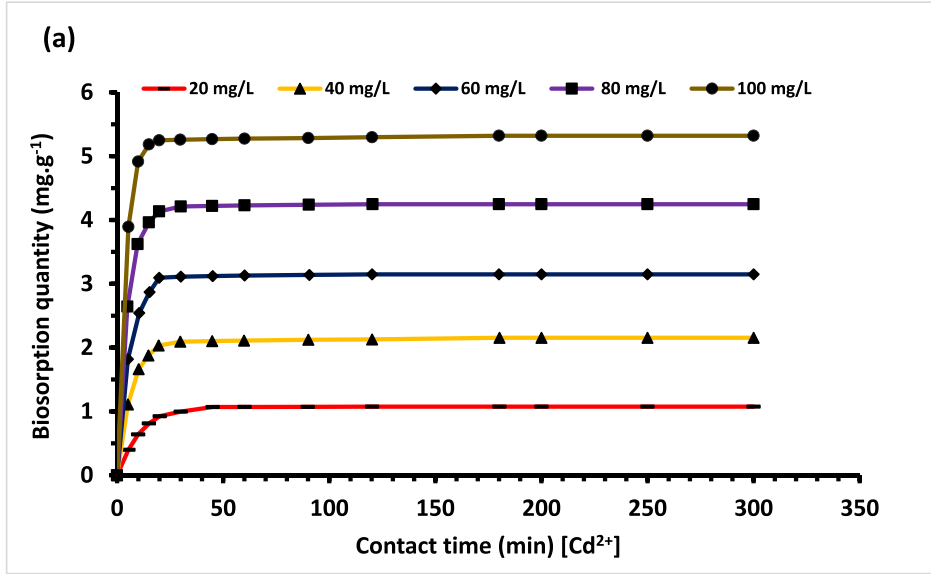

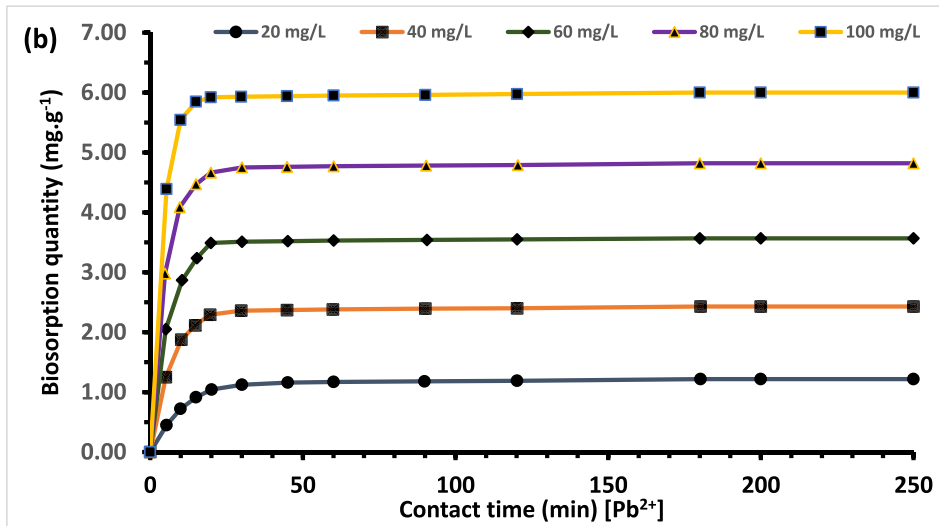

Fig. 12 Effect of contact time on biosorption capacity to *Acacia Gummifera* biomass of (a) Cd^{2+} and (b) Pb^{2+}. Experimental conditions: biosorbent dosage = 0.8 g; contact time: 300 min, temperature 303 K, pH = 6.5.

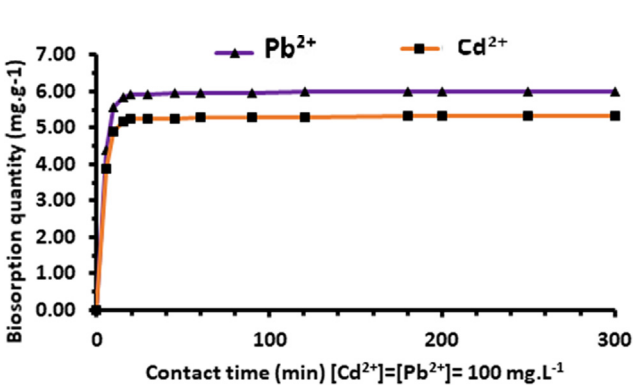

Fig. 13 Comparison between Pb^{2+} and Cd^{2+} biosorption on *Acacia Gummifera* using 0.8 g biosorbent and 100 mg/L metal concentration at pH 6.0.

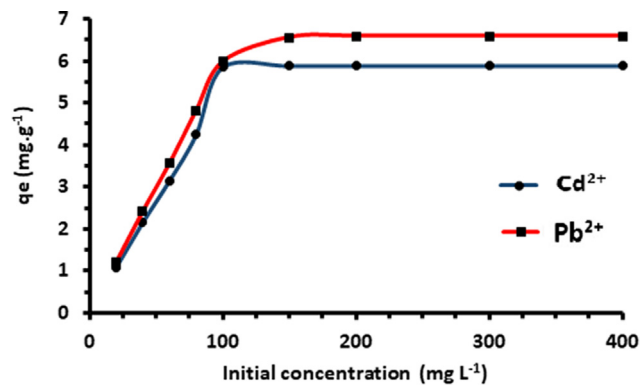

Fig. 14 Biosorption equilibrium of *Acacia Gummifera* at different initial Pb^{2+} and Cd^{2+} concentrations. Experimental conditions: Biosorbent mass 0.8 g, pH 6.5 and contact time 400 min.

$$\log(q_e - q_t) = \log(q_e) - [\frac{k_1 t}{2.303}] \quad (7)$$

The values of (k_1) and (q_e) were computed from the slope of the linear plot of log (q_e-q_t) versus (t) (Table 1).

The pseudo second-order rate model was also determined from the plot of $\frac{1}{q_t}$ versus t which is given in the following formula (Ho and McKay, 1998):

$$\frac{dq_t}{dt} = k_2(qe - qt)^2 \quad (8)$$

Where k_2 (mg.g^{-1}.min^{-1}) is the second-order rate constant, q_t (mg.g^{-1}) is the amount of biosorption time t(min) and q_e is the amount of biosorption equilibrium (mg.g^{-1}).

After integration and applying limiting conditions t = 0 to t = t and, q = 0 to q = q_t, the following equation (9) is obtained:

$$\frac{t}{q_t} = \left[\frac{1}{(k_2 q_e^2)}\right] + \frac{t}{q_e} \quad (9)$$

Where $k_2 q_e^2$ is the initial sorption rate when t = 0. The plot t/q_e versus t shows a linear relationship allowing computation of q_e and k_2.

It is interesting to consider intercepts of these pseudo-second order kinetic plots, because they allow determining the initial adsorption rate h (mg.g^{-1}.min^{-1}) at the beginning of the adsorption process (Ho and McKay, 1998). h is calculated as follows:

$$h = \frac{1}{k q_{max}^2} \quad (10)$$

Depending on the initial adsorption rate value (h), the mass transfer at the starting point of the process is greater for very low concentration then decreases with the increase in the initial concentration of metal ions. This phenomenon can be attributed to external resistance to mass transfer which seems to be the adsorption rate controlling step, and which will lead to chemisorption (thermodynamic control).

Adsorption kinetics for Pb^{2+} and Cd^{2+} are shown in Fig. 15. It was found that the adsorption of both metal ions onto *Acacia Gummifera* increases rapidly during the first 10 min, then increased slowly until reaching equilibrium (at t = 15 min). The experimental data were best fitted with pseudo-second-order model, with the highest coefficients of determination for both metal ions, as shown in Table 1 (R^2 > 0.999). The pseudo-second-order models showed good fits for all adsorption kinetic curves. The lowest HYBRID and MPSD values were close to zero, which indicated a better fit for adsorption kinetics (Table 1).

However, it can be noted that pseudo-first-order model had the lowest R^2 values and differed significantly from experimental data, suggesting that the biosorption doesn't follow a pseudo-first-order reaction. Both facts suggest that the pseudo-second-order model is more likely to predict kinetic behavior for the whole time range, which relies on the assumption that the rate-limiting step might be an electrostatic attraction through chemical sorption in a monolayer onto its surface.

It is essential to assess whether the kinetic models of the pseudo-first and second-order control properly the kinetic process when there is a possibility that adsorbate species diffuse into the adsorbent pores. In this case, the diffusion mechanism will have a significant effect on the kinetic model controlling the adsorption. The initial rate of the intraparticle diffusion can be obtained from Equation (11) (Weber and Chakravorti, 1974):

$$q_t = k_{id} t^{\frac{1}{2}} + b \quad (11)$$

Where k_{id} is the intraparticle diffusion rate constant (mg.g^{-1}.min$^{0.5}$). The value of the intercept b provides an idea of the thickness of the boundary layer. The plot of q_t as a function $t^{0.5}$ represented in Fig. 16 gives multilinear lines showing a two-step diffusion process for all studied concentrations. The first linear lines represent the instantaneous adsorption on the external surface. The second part of the plot represents the step of intraparticle diffusion which represents the limiting step of the adsorption mechanism. Diffusion rate constants are calculated using equation (11). As expected, the diffusion rate

Table 1 Pseudo-first-order, pseudo-second-order and intraparticle diffusion for the biosorption of Pb^{2+} and Cd^{2+} onto gum of *Acacia Gummifera*.

Metal ion	Initial metal ion concentration (mg. L^{-1})	Pseudo-first-order					Pseudo-second-order					
		K_1(min^{-1})	qe (mg. g^{-1})	R^2	HYBRID	MPSD (p)	K2 (mg. g^{-1}. min^{-1})	qe (mg. g^{-1})	R^2	h (mg. g^{-1}min^{-1})	HYBRID	MPSD (p)
Pb^{2+}	20	0.09	0.987	0.983	1.859	3.218	0.092	1.167	0.996	7.97	10.83	18.75
	40	0.16	2.279	0.958	15.350	26.582	0.132	2.119	0.997	1.68	5.643	9.769
	60	0.211	1.960	0.800	41.341	71.568	0.146	3.105	0.997	0.71	4.709	8.105
	80	0.210	2.463	0.893	3.045	5.272	0.143	4.09	0.998	0.42	2.350	4.068
	100	0.103	0.138	0.482	131.657	227.92	0.228	5.020	0.999	0.11	1.236	2.141
Cd^{2+}												
	20	0.08	0.945	0.945	1.125	1.948	0.086	1.180	0.988	8.31	9.095	15.746
	40	0.13	1.940	0.969	6.115	10.586	0.115	2.160	0.991	1.85	5.418	9.380
	60	0.11	1.044	0.849	29.73	51.580	0.118	3.140	0.994	0.85	3.312	5.734
	80	0.113	1.385	0.995	21.31	36.905	0.121	4.130	0.996	0.48	1.879	3.250
	100	0.273	0.900	0.932	17.37	30.080	0.185	5.072	0.997	0.21	1.130	1.956

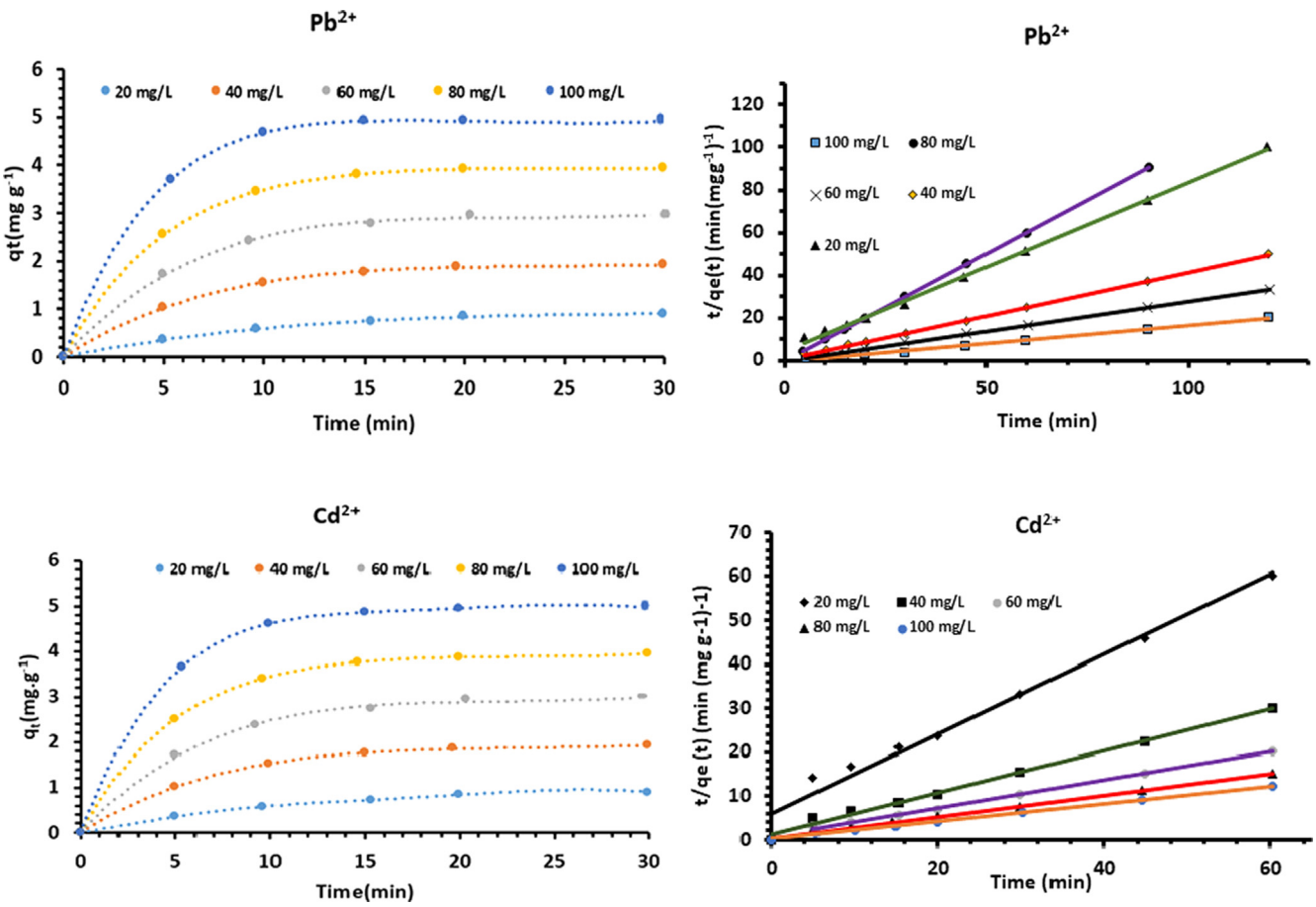

Fig 15 Experimental kinetic data and pseudo second order kinetics for Pb^{2+} and Cd^{2+} adsorption on *A. Gummifera*.

constant (k_{id1}) in the first step is higher than in the second step (k_{id2}).

The metal ions were first adsorbed by the external surface with a k_{id1} value ten times greater than k_{id2}, suggesting that the adsorption process was controlled by the boundary layer (film) diffusion. Values of diffusion constants k_{id1} and k_{id2} were computed from the slope of each plot. Table 2 shows the intraparticle diffusion constants (k_{id1} and k_{id2}) at different metal ions concentrations. The mechanism of diffusion has two distinct phases with higher R^2 values for the second phase (k_{id2}). These results suggest that the intraparticle diffusion is the rate determining step.

Once the outer surface is completely saturated, metal ions diffuse into the internal pores and get adsorbed by the inner adsorbent surface. When metal ions diffuse through the internal pores or along the pores' wall surface, the resistance to diffusion increases, which results in a decrease of the diffusion rate.

To sum up, the analysis of kinetic modeling results suggests that film diffusion controls the early biosorption steps, while the electrostatic interaction step plays the most important role in the removal of the metal ions.

Based on the Weber-Morris approach, it can be concluded that both film and intra-particle diffusion processes are involved in controlling the rate of adsorption.

3.7. Biosorption isotherm modeling

The sorption capacity of *Acacia Gummifera* can be determined from equilibrium sorption isotherm, which expresses the affinity and surface properties of *Acacia Gummifera*. In this case, it is a simple application of the law of mass action leading to the thermodynamic equilibrium constant K_0 defined as below (equation (12)) (Liu, 2009).

$$K_0 = \frac{(a_{complex})_{eq}}{(a_{freesites})_{eq}(a_{solute})_{eq}} \tag{12}$$

Where K_0 is a thermodynamic equilibrium constant, $(a_{complex})_{eq}$ is the complex activity, $(a_{free\ sites})_{eq}$ is the activity of free sites and $(a_{solute})_{eq}$ is the activity of solutes at equilibrium.

In the present study, we have chosen to fit the experimental data to Langmuir, Freundlich, Temkin and Dubinin–Radushkevich isotherm models.

3.7.1. Langmuir isotherm

The Langmuir sorption model has been successfully applied to the biosorption process of the studied metal ions. The Langmuir theory assumes that the sorption takes place at specific homogenous sites within the sorbent.

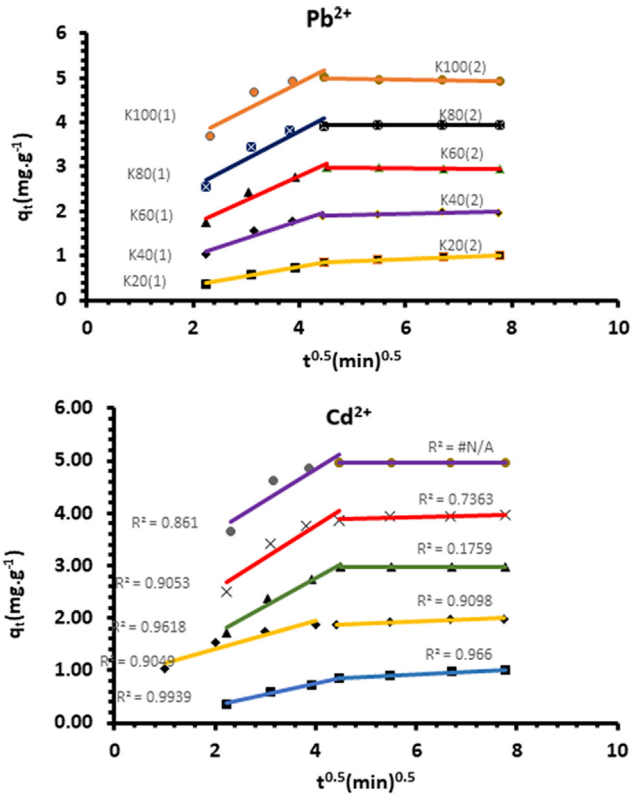

Fig. 16 Intraparticulate diffusion model for the biosorption of Pb^{2+} and Cd^{2+} ions onto *Acacia Gummifera*.

The linear form of Langmuir isotherms commonly cited in the literature (Foo and Hameed, 2010; Farouq and Yousef, 2015; Song et al., 2014; Ng et al., 2002) is the following:

$$\frac{1}{q_e} = \frac{1}{q_m} + \frac{1}{bC_e q_m} \tag{13}$$

Where q_m is the monolayer biosorption capacity of the adsorbent, expressed in $mg.g^{-1}$; q_e is the metal ion concentration sorbed per sorbent mass unit at equilibrium, expressed in $mg.g^{-1}$; b is the Langmuir sorption constant, expressed in $L.mg^{-1}$ commonly named K_L; and C_e is the equilibrium metal ion concentration in the residual solution, expressed in $mg.L^{-1}$.

The values of K_L and q_m were obtained using the slope, the intercept, $1/q_m$ and $1/(K_L.q_m)$ from the plot 1 /qe versus 1/Ce, and compared with the experimental data. Correlation coefficients as well as relative error values of hybrid fractional error function (HYBRD) and Marquardt's percent standard deviation (MPSD) for the linear forms of the Langmuir isotherms are summarized in Table 1. It appears that biosorption capacity varies greatly depending on biosorption conditions. For Pb^{2+}, the highest biosorption obtained was around 18 mg/g, whereas it didn't exceed 9 mg/g for Cd^{2+}. Langmuir isotherm plots (Fig. 17) illustrating the biosorption of Pb^{2+} and Cd^{2+} onto *Acacia Gummifera* biomass show that the experimental values were well fitted with Langmuir isotherm model. A high degree of correlation was obtained for both metal ions ($R^2 > 0.995$) (table 1), which suggests a chemical adsorption in a monolayer on the surface of the biosorbent. Adsorption process could have involved electrostatic interactions between metal ions and functional groups such as hydroxyl and carboxyl functions identified in *Acacia Gummifera* FTIR spectrum (Fig. 2).

Langmuir constant for Pb^{2+} and Cd^{2+} ions increased with rising temperature from approximately 0.12 to 0.24 $L.mg^{-1}$ and 0.01 to 0.11 $L.mg^{-1}$, respectively. The separation factor, commonly called equilibrium parameter R_L is the main parameter indicating the feasibility of the Langmuir isotherm. R_L is defined by the following relationship (Weber and Chakravorti, 1974):

$$R_L = \frac{1}{1 + K_L C_0} \tag{14}$$

Where C_0 is the initial concentration ($mg.L^{-1}$) and b is the Langmuir equilibrium constant ($L.mg^{-1}$). Depending on the value of the separation parameter (R_L), the adsorption conditions can be favorable or not (Chen, 2013):

If $R_L > 1$ Langmuir isotherm indicates that adsorption is not favored;
If $R_L < 1$ Sorption is favored;
If $R_L = 0$ Sorption is irreversible.

As shown in table 3, the dimensionless separation factor of both Pb^{2+} and Cd^{2+} ions is less than 1, indicating that *Acacia Gummifera* is a suitable biosorbent for the biosorption of Pb^{2+}

Table 2 Diffusion constants parameters for biosorption of Pb^{2+} and Cd^{2+} onto *Acacia Gummifera*.

Metal ion	C_i: Initial concentration ($mg.L^{-1}$)	$k_{id(1)}(C_i)$ ($mg.g^{-1}.min^{0.5}$)	bi	R^2	$k_{id(2)}(C_i)$ ($mg.g^{-1}.min^{0.5}$)	bi	R^2
Pb^{2+}	20	0.22	0.05	0.994	0.05	0.65	0.957
	40	0.39	0.03	0.964	0.03	1.77	0.857
	60	0.54	−0.01	0.905	0.01	3.04	0.885
	80	0.62	0.01	0.905	0.01	3.90	0.409
	100	0.60	0.02	0.861	0.02	5.11	0.837
Cd^{2+}	20	0.22	−0.11	0.994	0.05	0.63	0.966
	40	0.27	0.86	0.905	0.04	1.71	0.910
	60	0.54	0.61	0.962	0.00	2.95	0.175
	80	0.61	1.31	0.905	0.02	3.78	0.736
	100	0.60	2.46	0.862	0.00	4.95	nd

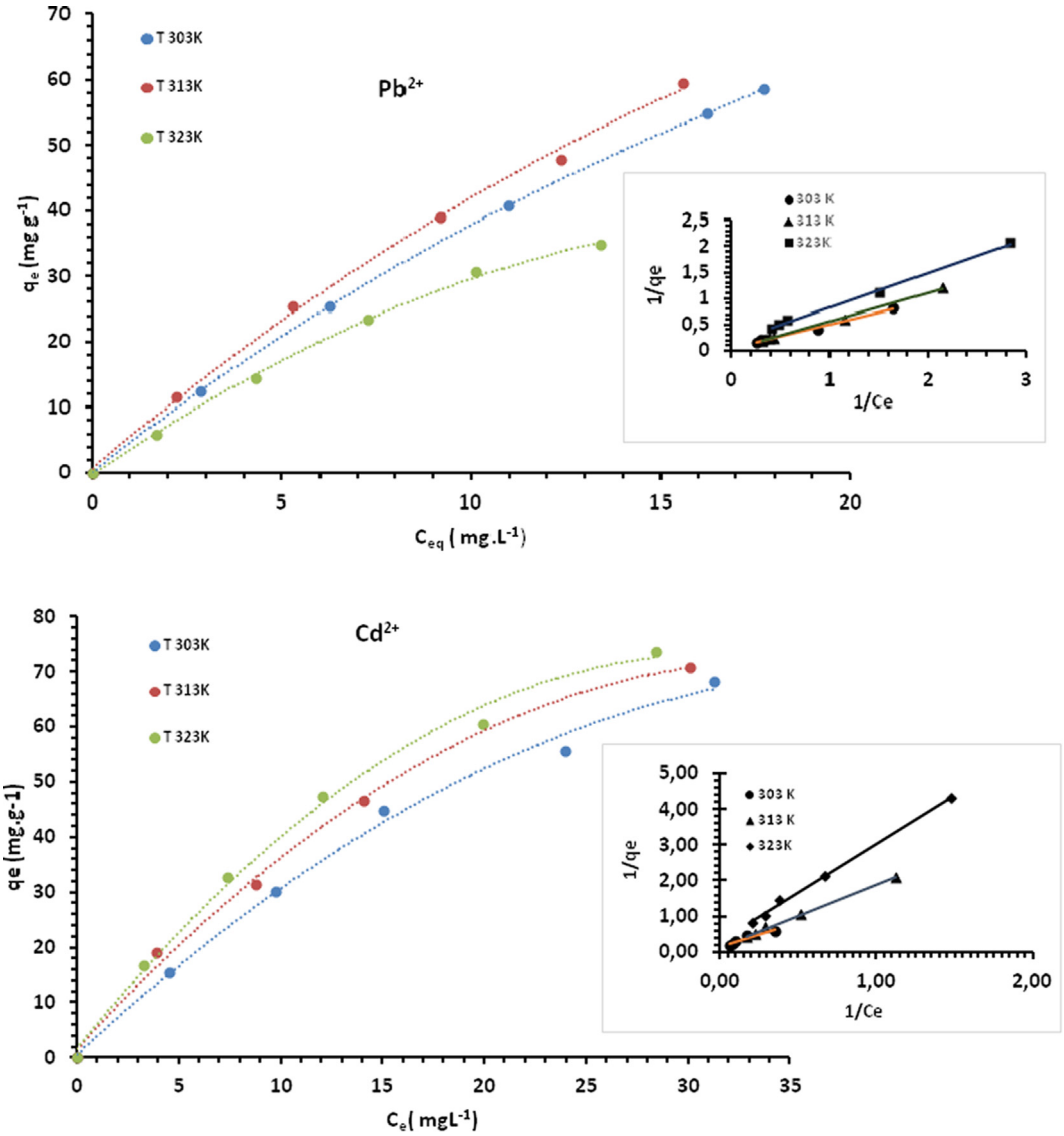

Fig. 17 Sorption isotherms onto *Acaia Gummifera* biomass with linear form by the Langmuir isotherm model at different temperatures.

and Cd^{2+} and probably of irreversible nature for Cd^{2+} (R_L = 0.077 at 303 K).

3.7.2. Freundlich isotherm

Freundlich isotherm is an empirical equation commonly used to describe the distribution of adsorption energy onto heterogeneous surface of the adsorbent (Freundlich, 1907). The linearized form of Freundlich model (Brouers and Al-Musawi, 2015) is:

$$log\ q_e = \frac{1}{n} log\ C_e + log\ K_F \quad (15)$$

Where K_F and n are the Freundlich constants related respectively to the adsorption capacity and intensity of biosorption. The results obtained are represented according to the Freundlich model, by plotting log (qe) versus log (Ce). n is calculated as the slope of the line and log K_F the ordinate at the origin (Fig. 18).

Values of Freundlich isotherm parameters and coefficient of determination (R^2) at different temperatures are shown in Table 3. The maximum K_F determined was found to be 1.56 $mg.g^{-1}$ for Pb^{2+} at 303 K and 1.24 $mg.g^{-1}$ at 323 K for Cd^{2+}. Meanwhile, the coefficient of determination values (R^2) was found to be less for the Freundlich model in comparison to the Langmuir model. The obtained n values (Table 3) were greater than 1.0, which indicated a favorable Pb and Cd bioadsorption process. According to the linear regression factor R^2 (Table 3), both Langmuir and Freundlich models showed good agreement with experimental results. However, even if Langmuir isotherm model had a better fit for the experimental data (R^2-1), high R^2 values obtained with Freundlich model may indicate a possible concomitant physisorption mechanism.

3.7.3. Dubinin–Radushkevich (D-R) isotherm

The D-R isotherm model is based on the assumption that the adsorption potential is related to micropore volume filling,

Table 3 Parameters of q_{max} and K_L in Langmuir isotherm and K_F and $1/n$ in Freundlich isotherm for the biosorption of pb^{2+} and Cd^{2+} onto *Acacia Gummifera*.

Metal ions	Temp (K)	Langmuir						Freundlich					
		qm(mg. g^{-1})	K_L(L. mg^{-1})	R^2	R_L	HYBRD	MPSD	K_F(mg. g^{-1})	1/n	n	R^2	HYBRD	MPSD
Pb^{2+}	303	18.3	0.12	0.989	0.077	0.248	0.429	1.56	0.954	1.05	0.984	0.059	0.119
	313	12.9	0.19	0.993	0.051	0.206	0.356	2.08	0.781	1.28	0.979	2.237	3.873
	323	6.3	0.24	0.996	0.039	0.341	0.591	0.93	0.605	1.33	0.740	20.557	35.587
Cd^{2+}	303	9.6	0.01	0.997	0.481	0.122	0.211	0.42	0.917	1.09	0.996	0.049	0.086
	313	7.6	0.08	0.997	0.117	0.285	0.493	1.14	0.602	1.66	0.989	0.060	0.104
	323	3.4	0.11	0.997	0.085	0.593	1.026	1.24	0.554	1.80	0.985	0.153	0.265

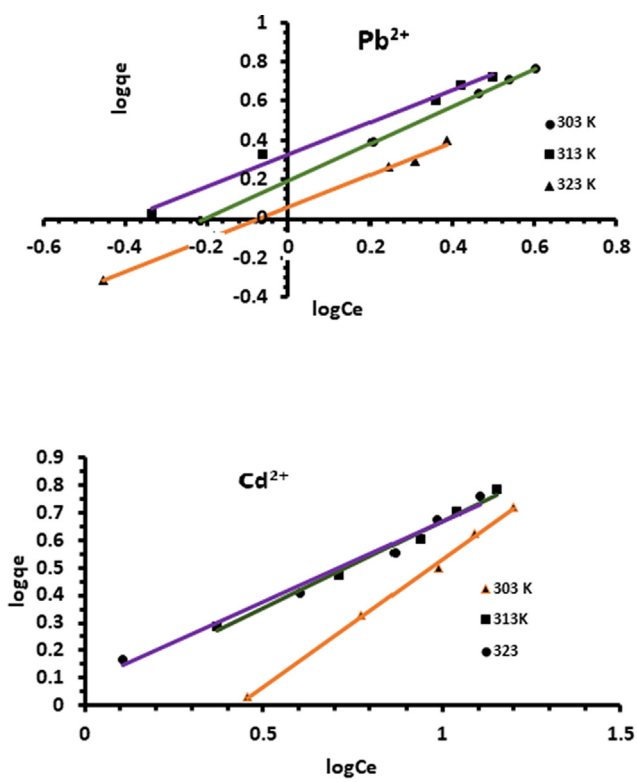

Fig. 18 Freundlich isotherm plot for the adsorption of Pb^{2+} and Cd^{2+} onto *Acacia Gummifera* biomass.

since the adsorption surface is not assumed to be homogeneous (Kaur et al., 2015). This model is the opposite of Langmuir's theory which assumes that sorption is based on the filling of the volume of micropores layer by layer, on the walls of the pores (Inglezakis, 2007). The linearized form of the D-R isotherm model (Togue Kamga, 2018) is expressed as:

$$ln\ q_e = log\ q_s - K_{ads}\varepsilon^2 \tag{16}$$

where qs is the theoretical saturation capacity of the isotherm ($mg.g^{-1}$); qe is the amount of adsorbate per adsorbent mass unit at equilibrium (mg/g); K_{ads} is the Dubinin–Radushkevich isotherm constant ($mol^2.J^{-2}$) related to the adsorption energy; and ε = Dubinin–Radushkevich isotherm constant is the adsorption potential. D-R constants were deduced from the isotherm plot (Fig. 19) as the slope and the intercept (Table 4).

Mean free energy (E) per molecule of adsorbate can be computed by the following relationship (Dubinin, 1960):

$$E = \frac{1}{\sqrt{2K_{ads}}} \tag{17}$$

The parameter ε is defined by the following relationship:

$$\varepsilon = RT\ Ln\left(1 + \frac{1}{C_e}\right) \tag{18}$$

where R is the gas constant (8.314 $J.mol^{-1}.K^{-1}$), T is the absolute temperature (K) and Ce characterizes adsorbate equilibrium concentration ($mg.L^{-1}$).

One of the drawbacks of Dubinin–Radushkevich isothermal model is that it does not take into account the influence of the solvent, especially the effect of the pH of the solution and the dissociation of the functional groups on the sorbent surface, since the model was proposed to describe the adsorption of a solute at the solid absorbent/gas interface. Nevertheless, the model can provide average free energy with lower precision to distinguish physical or chemical adsorption in a solid / solution adsorption system.

q_s values obtained from the linear plot of Dubinin–Radushkevich model were 5.44 $mg.g^{-1}$ for Pb^{2+} and 5.08 $mg.g^{-1}$ for Cd^{2+}. The mean free energy (E) obtained for Pb^{2+} and Cd^{2+} were 1.38 and 0.51 $KJ.mol^{-1}$, respectively

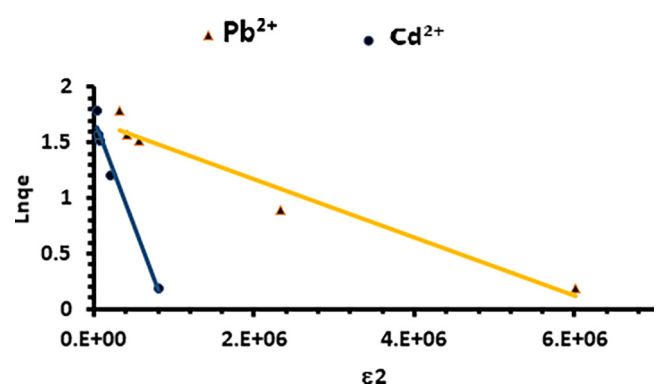

Fig. 19 Dubinin–Radushkevich equilibrium adsorption isotherm of the experimental data.

Table 4 Dubinin–Radushkevich isotherm constants for the adsorption of Pb^{2+} and Cd^{2+} onto *Acacia Gummifera* biomass.

Metal Ion	Temp (K)	Dubinin–Radushkevich isotherm					
		q_s (mg.g^{-1})	K_{ad} (mol^2/J^2)	E(KJ.mol^{-1})	R^2	HYBRID	MPSD(%)
Pb^{2+}	303	5.44	$2.6.10^{-7}$	1.38	0.956	2.973	5.15
Cd^{2+}	303	5.08	$5.66.10^{-5}$	0.51	0.905	6.88	11.92

(Table 4). Bonding energies for ion-exchange mechanism have been reported to range between 8 and 16 kJ/mol (Helfferich, 1962). It is also admitted that in physisorption process involving electrostatic interaction between charged particles, binding energy ranges between 0 and −20 kJ.mol^{-1} (Jaycock and Parfitt, 1981), whereas values more negative than −40 kJ.mol^{-1} indicate a chemisorption process (Zafar et al., 2007). E values (1.38 and 0.51 KJ.mol^{-1} < 8 KJ/mol) obtained in this study indicate that physical adsorption would play a significant role in the sorption process of the metal ions on *Acacia Gummifera*.

The coefficient of determination (R^2 > 0.905) is significantly lower than that obtained with Langmuir model (R^2 > 0.989) for both metal ions. The constants, qs and K_{ads} obtained for Dubinin–Radushkevich isotherm model were around 5 mg.g^{-1} and 10^{-6} mol^2.J^{-2}, which is low in comparison to Langmuir model (18 mg.g^{-1}).

3.7.4. Temkin isotherm

The interactions between adsorbent and adsorbate are taken into account in Temkin model, which assumes that the sorption free energy is a function of the surface coverage (Temkin and Pyzhev, 1940). It is an application of the Gibbs equation for the determination of adsorption energy. It assumes that the pollutant molecules are retained energetically in a homogeneous way on the surface of the adsorbent (Ofomaja, 2008). Although this isotherm is usually used for adsorption of gases on solids, several researchers proposed to use this model for the determination of adsorption energy variation in a liquid phase, by plotting (qe) as a function of LnCe (Temkin and Pyzhev, 1940; Aharoni and Ungarish, 1977). The model of Temkin isotherm is:

$$q_e = \left(\frac{RT}{b}\right) \ln (A_T C_e) \tag{19}$$

$$q_e = B_T \ln (A_T) + B_T \ln (C_e) \tag{20}$$

And

$$B_T = \frac{RT}{b_T} \tag{21}$$

Where Ce is the adsorbate concentration at equilibrium (mg.L^{-1}), A_T is Temkin isotherm equilibrium binding constant (L.g^{-1}), corresponding to the maximum bonding energy; b_T is Temkin isotherm constant, related to the variation of adsorption energy in (J.mol^{-1}) and to bonding energy; R is universal gas constant (8.314 J.mol^{-1}.K^{-1}); T is the temperature (298 K) and; B_T is a constant related to the heat of sorption (J.mol^{-1}).

The plots of qe versus lnCe (Fig. 20) are used to determine B_T and A_T values. b_T values which give an indication of the heat of sorption were calculated using equation (21) and depicted in Table 5. All b_T values were between 9.56 and 19.15 KJ.mol^{-1}, suggesting a physical adsorption process due to electrostatic interaction between the positively charged metal ions and the negatively charged surface after deprotonation of glucuronic acid and 4-O-methylglucuronic acid contained in AGPs of Acacia gum (Showalter, 2001). These results are in accordance with Dubinin–Radushkevich isotherm predictions.

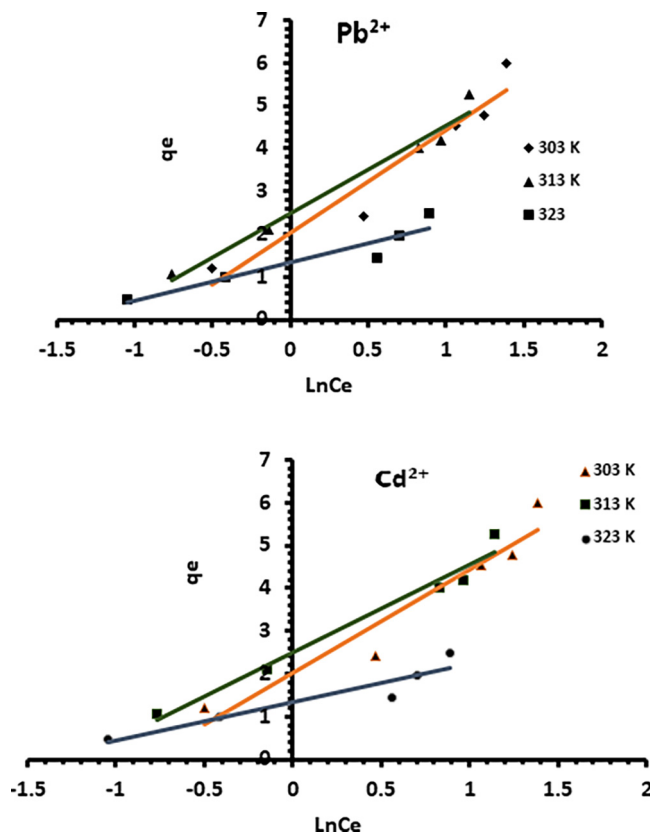

Fig. 20 Equilibrium adsorption isotherm of the experimental isotherms according to Temkin model.

The variation of adsorption energy b_T resulting from the linearization of Temkin model is always positive for the two metals. These results suggest that the adsorption of the metal mixture on *Acacia Gummifera* biomass is exothermic. However, Langmuir and Freundlich's models showed better correlation coefficients ($R^2 \approx 1$) and lower HYBRID and MPSD error values than Temkin model (Fig. 20).

Four adsorption isotherm models were examined in this study; investigation of the biosorption equilibrium was carried out at three temperatures 303, 312 and 323 K except for Dubinin–Radushkevich model, studied only at 303 K. The sorption data were well fitted with Langmuir, Freundlich, Temkin and

Table 5 Temkin isotherm constants for the adsorption Pb^{2+} and Cd^{2+} onto *Acacia Gummifera* biomass.

Metal Ion	Temp (K)	Temkin isotherm				
		A_T (L.mg^{-1})	b_T (KJ.mol^{-1})	R^2	HYBRID	MPSD(%)
	303	6.98	19.15	0.920	1556	269
Pb^{2+}	313	16.73	15.90	0.972	974	1688
	323	323.45	33.08	0.791	124	302
Cd^{2+}	303	6.98	10.05	0.924	1340	258
	313	16.74	9.72	0.972	843	241
	323	32.55	9.56	0.887	1782	320

Dubinin–Radushkevich models. A good correlation was found between experimental data and Langmuir's isotherm, suggesting a chemical monolayer adsorption. The results obtained with Dubinin–Radushkevich and Temkin's models indicated that physical interactions could also contribute to the biosorption process.

The results of this work demonstrated that *Acacia Gummifera* biomass is an effective adsorbent for the removal of lead and cadmium from aqueous solutions.

3.8. Biosorption thermodynamics

A thermodynamic study has been undertaken to determine the spontaneous nature of the adsorption process and its feasibility (see supplementary material).

The results indicate a physical and exothermic adsorption Furthermore, negative ΔS^0 (Pb^{2+},Cd^{2+}) values indicate the formation of more stable *Acacia Gummifera*-Pb^{2+} and *Acacia Gummifera*-Cd^{2+} complexes.

3.9. Comparison of biosorption capacity for Cd^{2+} and Pb^{2+} of A. Gummifera biomass with some adsorbents reported in the literature

The biosorption capacity of *Acacia Gummifera* for Pb^{2+} and Cd^{2+} was compared with other biosorbents reported in the literature (Table 6).

The empirical data obtained in the present study are consistent with the results reported by Manawi et al. (2018) who studied lead removal from water using Acacia Gum. However, the adsorption capacity of *Acacia Gummifera* in the present study was found to be higher than that reported by Waseem et al. (2014) who studied the elimination of Pb^{2+} and Cd^{2+} ions from aqueous solutions using *Acacia Nilotica*. This difference can be explained by the variation of the biochemical composition and molecular characteristics of the Acacia Gum, which can be affected by internal and external factors such as Acacia species, age of trees and weather conditions (Siddig et al., 2005). Also, this relatively weak adsorption could be explained by the high ratio between the biomass and the metal ion concentrations which amounts to − 1/100, as high biomass concentration restricts the access of metal ions to the binding sites.

On the other hand, Pehlivan et al. (2008) reported higher biosorption capacity of sugar beet pulp for both metal ions (Table 6). This may be due to the weaker acidic groups of carboxyl functions of galacturonic acid in pectic substances (> 40% of the dry matter) from sugar beet pulp which are known to strongly bind metal cations in solution (Pehlivan et al., 2008). Moreover, we can note from table 6 that, compared with Acacia species, Algae biomass showed high biosorption capacity for cadmium and lead cations (Abdel-Aty et al., 2013). This is may be due to potential metal cation-binding sites of algal cell components, including numerous chemical functional groups (carboxyl, amine, imidazole, phosphate, imidazole sulfhydryl and hydroxyl) entering into the structure of cell proteins and carbohydrates. Nevertheless, there are some challenges for using algae as biosorbent, including sourcing, production management and availability, given the increasing demand in the pharmaceutical and cosmetic fields. For this reason, it is imperative to look for an alternative low cost and highly selective biosorbent to eliminate metal ions from water. In this study, we propose the *Acacia Gummifera* as a promising non-conventional low cost biosorbent for the elimination of Pb^{2+} and Cd^{2+} ions from aqueous solutions.

Table 6 Comparison of biosorption capacity qm (mg.g^{-1}) for Cd^{2+} and Pb^{2+} of *A. Gummifera* biomass with other adsorbents.

Biosorbent	Cd^{2+}	Pb^{2+}	Reference
Aloe Vera wastes	104.2	–	Noli et al., 2019
Alga Anabaena Sphaerica biomass	111.1	121.95	Abdel-Aty et al., 2013
Sugar beet pulp	46.1	43.5	Pehlivan et al., 2008
Acacia Nilotica	4.99	2.51	Waseem et al., 2014
Acacia gum	–	12.2	Manawi et al., 2018
Acacia Gummifera gum powder	9.57	18.3	Present study

4. Conclusion

This study highlighted the possibility of using *Acacia Gummifera* as an alternative adsorbent for the simultaneous removal of Pb^{2+} and Cd^{2+} ions from aqueous solutions using

the batch sorption technique. The influence of parameters related to operating conditions such as contact time, biosorbent dosage, pH, initial metal ions concentrations and temperature was examined.

Experimental data were data were well-fitted with Langmuir isotherm model (R^2-1). The sorption mechanism was found to be based on the interaction of specific active sites on the surface of Acacia with the monolayer of metal ions. Negative change ΔS^0 values indicated that stable *Acacia*-Pb^{2+} and *Acacia*-Cd^{2+} complexes were formed following adsorption. The ΔG^0 values in the adsorption process of both Cd^{2+} and Pb^{2+} ions on *Acacia* were found to be negative, which suggests a spontaneous adsorption of the metal ions on the biosorbent.

The adsorption process onto *Acacia Gummifera* has been found to involve the mechanism of electrostatic interaction. The maximum removal efficiencies were obtained at pH 6.5 and reached 97% and 86% respectively for Pb^{2+} and Cd^{2+}, with a maximum monolayer biosorption capacity of 18.3 mg.g^{-1} and 9.57 mg.g^{-1} for Pb^{2+} and Cd^{2+}, respectively. Physical interactions involvement in the biosorption process has been confirmed by Dubinin–Radushkevich and Temkin models. These models show some heterogeneity of adsorption sites. Biosorption kinetics was studied using pseudo-first order, pseudo-second order and intraparticle diffusion. Results obtained with biosorption kinetics show clearly the adequacy of pseudo–second order model, which provides the best fit to adsorption kinetic for Cd^{2+} and Pb^{2+} ions onto *Acacia Gummifera*, with correlation coefficient values close to unity, and the lowest HYBRID and MPSD error values (close to zero), indicating that chemical sorption prevails over physisorption. The kinetic study suggested that in the early stages, the adsorption rate was firstly controlled by film diffusion, and later by pore diffusion. This result implies that the dominant process is chemisorption. Competitive adsorption experiment indicated that *Acacia Gummifera* had a stronger affinity to Pb^{2+} than to Cd^{2+}. This is probably due to their different hydrated ionic radii. SEC-HPLC analysis showed that the glycoproteins entering into the structure of *Acacia Gummifera*, particularly AGP and AG, seem to be the major components involved in the biosorption process. Covalent bonding and ionic bonding could occur respectively between metal ions and amino groups and with carboxyl groups.

These findings suggest that *Acacia Gummifera* could be an effective low-cost biosorbent for the removal of lead and cadmium from contaminated effluents.

Declaration of Competing Interest

The authors declare that they have no known competing financial interests or personal relationships that could have appeared to influence the work reported in this paper.

Acknowledgment

This work was supported by the Deanship of Scientific Research (DSR), King Abdulaziz University, Jeddah, Saudi Arabia, under grant No. (DF-747-155-1441). The authors, therefore, gratefully acknowledge the DSR technical and financial support.

Appendix A. Supplementary material

Supplementary data to this article can be found online at https://doi.org/10.1016/j.arabjc.2020.08.022.

References

Abdel-Aty, A.M., Ammar, N.S., Abdel Ghafar, H.H., Ali, R.K., 2013. Biosorption of cadmium and lead from aqueous solution by fresh water alga anabaena sphaerica biomass. J. Adv. Res. 4 (4), 367–374. https://doi.org/10.1016/J.JARE.2012.07.004.

Ahamed, M., Siddiqui, M.K.J., 2007. Low level lead exposure and oxidative stress: Current opinions. Clin. Chim. Acta 383, 57–64. https://doi.org/10.1016/j.cca.2007.04.024.

Aharoni, C., Ungarish, M., 1977. Kinetics of activated chemisorption. Part 2. —Theoretical models. J. Chem. Soc., Faraday Trans. 1 73, 456–464. https://doi.org/10.1039/F19777300456.

Allen, S.J., McKay, G., Porter, J.F., 2004. Adsorption isotherm models for basic dye adsorption by peat in single and binary component systems. J. Colloid Interface Sci. 280, 322–333. https://doi.org/10.1016/j.jcis.2004.08.078.

Malihe, Amini, Habibollah, Younesi, Nader, Bahramifar, 2013. Biosorption of U(VI) from Aqueous Solution by Chlorella vulgaris: Equilibrium, Kinetic, and Thermodynamic Studies. J. Environ. Eng. 139, 410–421. https://doi.org/10.1061/(ASCE)EE.1943-7870.0000651.

Anirudhan, T.S., Radhakrishnan, P.G., 2009. Kinetic and equilibrium modelling of Cadmium(II) ions sorption onto polymerized tamarind fruit shell. Desalination 249, 1298–1307. https://doi.org/10.1016/j.desal.2009.06.028.

Awuala, M.R., 2019. Mesoporous composite material for efficient lead (II) detection and removal from aqueous media. J. Environ. Chem. Eng. 7, 103124.

Awualb, M.R., 2019. Innovative composite material for efficient and highly selective Pb(II) ion capturing from wastewater. J. Mol. Liq. 284, 502–510.

Awual, M.R., Hasan, M.M., Islam, A., Rahman, M.M., Asiri, A., Khaleque, M.A., Sheikh, M.C., 2019. Offering an innovative composited material for effective lead(II) monitoring and removal from polluted water. J. Cleaner Prod. 231, 214–223.

Ayoob, S., Gupta, A.K., 2008. Insights into isotherm making in the sorptive removal of fluoride from drinking water. J. Hazard. Mater. 152, 976–985. https://doi.org/10.1016/j.jhazmat.2007.07.072.

Baig, J.A., Kazi, T.G., Shah, A.Q., Kandhro, G.A., Afridi, H.I., Khan, S., Kolachi, N.F., 2010. Biosorption studies on powder of stem of Acacia nilotica: Removal of arsenic from surface water. J. Hazard. Mater. 178, 941–948. https://doi.org/10.1016/j.jhazmat.2010.02.028.

Barth, A., Zscherp, C., 2002. What vibrations tell about proteins. Q. Rev. Biophys. 35, 369–430. https://doi.org/10.1017/S0033583502003815.

Bernard, A., 2008. Cadmium & its adverse effects on human health. Ind. J. Med. Res. 128 (4), 557–564.

Bouazizi, S., Jamoussi, B., Bousta, D., 2016. Application of response surface methodology for optimization of heavy metals biosorption on natural gum of acacia nilotica. Int. J. Eng. Res. Technol. 5.

Brouers, F., Al-Musawi, T.J., 2015. On the optimal use of isotherm models for the characterization of biosorption of lead onto algae. J. Mol. Liq. 212, 46–51. https://doi.org/10.1016/j.molliq.2015.08.054.

Chen, C., 2013. Evaluation of equilibrium sorption isotherm equations. Open Chem. Eng. J. 7.

Chen, L., Liu, J., Zhang, Y., Dai, B., An, Y., Yu, L. (Lucy), 2015. Structural, thermal, and anti-inflammatory properties of a novel pectic polysaccharide from alfalfa (Medicago sativa L.) stem. J.

Agric. Food Chem. 63, 3219–3228. https://doi.org/10.1021/acs.jafc.5b00494.

Dubinin, M.M., 1960. The potential theory of adsorption of gases and vapors for adsorbents with energetically nonuniform surfaces. Chem. Rev. 60, 235–241.

Duruibe, J., M.o.c, O., Egwurugwu, J.N., 2007. Heavy metal pollution and human biotoxic effects [WWW Document]. URL https://www.semanticscholar.org/paper/Heavy-metal-pollution-and-human-biotoxic-effects-Duruibe-M.O.C./56f5b680f3a7bc77011562be171-b0a59730ed77f (accessed 4.28.20).

Eze, S.O., Igwe, J.C., Dipo, D., 2013. Effect of particle size on adsorption of heavy metals using chemically modified and unmodified fluted pumpkin and broad-leafed pumpkin pods. Int. j. biol. chem. sci. 7 (2), 852–860. https://doi.org/10.4314/ijbcs.v7i2.40.

Farooq, U., Kozinski, J.A., Khan, M.A., Athar, M., 2010. Biosorption of heavy metal ions using wheat based biosorbents – A review of the recent literature. Bioresour. Technol. 101, 5043–5053. https://doi.org/10.1016/j.biortech.2010.02.030.

Farouq, R., Yousef, N.S., 2015. Equilibrium and kinetics studies of adsorption of copper (II) on natural biosorbent. Int. J. Chem. Eng. Appl. 6 (5), 319–324. https://doi.org/10.7763/IJCEA.2015.V6.503.

Foo, K.Y., Hameed, B.H., 2010. Insights into the modeling of adsorption isotherm systems. Chem. Eng. J. 156, 2–10. https://doi.org/10.1016/j.cej.2009.09.013.

Freundlich, H., 1907. Über die Adsorption in Lösungen. Z. Phys. Chem. 57U, 385–470. https://doi.org/10.1515/zpch-1907-5723.

Galedar, M., Younesi, H., 2013. Biosorption of Ternary Cadmium, Nickel and Cobalt Ions from Aqueous Solution onto Saccharomyces cerevisiae Cells: Batch and Column Studies. Am. J. Biochem. Biotechnol. 9, 47–60. https://doi.org/10.3844/ajbbsp.2013.47.60.

Gedam, A.H., Dongre, R.S., 2015. Adsorption characterization of Pb (ii) ions onto iodate doped chitosan composite: equilibrium and kinetic studies. RSC Adv. 5, 54188–54201. https://doi.org/10.1039/C5RA09899H.

Helfferich, F., 1962. Theories of ion-exchange column performance: a critical study. Angew. Chem., Int. Ed. Engl. 1, 440–453. https://doi.org/10.1002/anie.196204401.

Ho, Y.S., McKay, G., 1998. Sorption of dye from aqueous solution by peat. Chem. Eng. J. 70, 115–124. https://doi.org/10.1016/S0923-0467(98)00076-1.

Inglezakis, V.J., 2007. Solubility-normalized Dubinin-Astakhov adsorption isotherm for ion-exchange systems. Micropor. Mesopor. Mater. 103, 72–81. https://doi.org/10.1016/j.micromeso.2007.01.039.

Jaycock, M.J., Parfitt, G.D., 1981. Chemistry of Interfaces. Ellis Horwood Ltd., Chichester, England.

Kačuráková, M., Capek, P., Sasinková, V., Wellner, N., Ebringerová, A., 2000. FT-IR study of plant cell wall model compounds: pectic polysaccharides and hemicelluloses. Carbohydrate Polym. 43, 195–203. https://doi.org/10.1016/S0144-8617(00)00151-X.

Kamran, S., Shafaqat, A., Samra, H., Sana, A., Samar, F., Muhammad, B.S., Saima, A.B., Hafiz, M.T., Hafiz, M.T., 2013. Heavy Metals Contamination and what are the Impacts on Living Organisms. GJEMPS 2, 172–179 https://doi.org/10.15580/GJEMPS.2013.4.060413652.

Kaur, S., Rani, S., Mahajan, R.K., Asif, M., Gupta, V.K., 2015. Synthesis and adsorption properties of mesoporous material for the removal of dye safranin: Kinetics, equilibrium, and thermodynamics. J. Ind. Eng. Chem. 22, 19–27. https://doi.org/10.1016/j.jiec.2014.06.019.

Khosa, M.A., Shah, S.S., Feng, X., 2014. Metal sericin complexation and ultrafiltration of heavy metals from aqueous solution. Chem. Eng. J. 244, 446–456. https://doi.org/10.1016/j.cej.2014.01.091.

Kurniawan, T.A., Chan, G.Y.S., Lo, W.-H., Babel, S., 2006. Physico–chemical treatment techniques for wastewater laden with heavy metals. Chem. Eng. J. 118, 83–98. https://doi.org/10.1016/j.cej.2006.01.015.

Kuyucak, N., Volesky, B., 1988. Biosorbents for recovery of metals from industrial solutions. Biotechnol. Lett. 10, 137–142. https://doi.org/10.1007/BF01024641.

Lakherwal, D., 2014. Adsorption of heavy metals: a review. Int. J. Environ. Res. Dev. 4 (1), 41–48.

Lamport, D.T.A., Várnai, P., 2013. Periplasmic arabinogalactan glycoproteins act as a calcium capacitor that regulates plant growth and development. New Phytol. 197, 58–64. https://doi.org/10.1111/nph.12005.

Lanphear, Bruce P., Richard, Hornung, Jane, Khoury, Kimberly, Yolton, Peter, Baghurst, Bellinger, David C., Canfield, Richard L., Dietrich, Kim N., Robert, Bornschein, Tom, Greene, Rothenberg, Stephen J., Needleman, Herbert L., Lourdes, Schnaas, Gail, Wasserman, Joseph, Graziano, Russell, Roberts, 2005. Low-level environmental lead exposure and children's intellectual function: an international pooled analysis. Environ. Health Perspect. 113, 894–899. https://doi.org/10.1289/ehp.7688.

Lindholm-Lehto, P.C., 2019. Biosorption of heavy metals by lignocellulosic biomass and chemical analysis. BioResources 14, 4952–4995.

Liu, Y., 2009. Is the free energy change of adsorption correctly calculated?. J. Chem. Eng. Data 54 (7), 1981–1985. https://doi.org/10.1021/je800661q.

Manawi, Y., McKay, G., Ismail, N., Kayvani Fard, A., Kochkodan, V., Atieh, M.A., 2018. Enhancing lead removal from water by complex-assisted filtration with acacia gum. Chem. Eng. J. 352, 828–836. https://doi.org/10.1016/j.cej.2018.07.087.

Mejia Tamayo, V., Nigen, M., Apolinar-Valiente, R., Doco, T., Williams, P., Renard, D., Sanchez, C., 2018. Flexibility and hydration of amphiphilic hyperbranched arabinogalactan-protein from plant exudate: a volumetric perspective. Colloids Interfaces 2, 11. https://doi.org/10.3390/colloids2010011.

Munagapati, V.S., Yarramuthi, V., Nadavala, S.K., Alla, S.R., Abburi, K., 2010. Biosorption of Cu(II), Cd(II) and Pb(II) by Acacia leucocephala bark powder: Kinetics, equilibrium and thermodynamics. Chem. Eng. J. 157, 357–365. https://doi.org/10.1016/j.cej.2009.11.015.

Nejatzadeh-Barandozi, F., Enferadi, S.T., 2012. FT-IR study of the polysaccharides isolated from the skin juice, gel juice, and flower of Aloe vera tissues affected by fertilizer treatment. Org. Med. Chem. Lett. 2, 33. https://doi.org/10.1186/2191-2858-2-33.

Ng, J.C.Y., Cheung, W.H., McKay, G., 2002. Equilibrium studies of the sorption of Cu(II) ions onto Chitosan. J. Colloid Interface Sci. 255 (1), 64–74. https://doi.org/10.1006/jcis.2002.8664.

Noli, F., Kapashi, E., Kapnisti, M., 2019. Biosorption of uranium and cadmium using sorbents based on aloe vera wastes. J. Environ. Chem. Eng. 7, (2). https://doi.org/10.1016/J.JECE.2019.102985 102985.

Ofomaja, A.E., 2008. Kinetic study and sorption mechanism of methylene blue and methyl violet onto mansonia (Mansonia altissima) wood sawdust. Chem. Eng. J. 143, 85–95. https://doi.org/10.1016/j.cej.2007.12.019.

Özer, A., 2007. Removal of Pb(II) ions from aqueous solutions by sulphuric acid-treated wheat bran. J. Hazard. Mater. 141, 753–761. https://doi.org/10.1016/j.jhazmat.2006.07.040.

Pearson, R.G., 1963. Hard and soft acids and bases. J. Am. Chem. Soc. 85, 3533–3539. https://doi.org/10.1021/ja00905a001.

Pehlivan, E., Yanik, B.H., Ahmetli, G., Pehlivan, M., 2008. Equilibrium isotherm studies for the uptake of cadmium and lead ions onto sugar beet pulp. Bior. Technol. 99 (9), 3520–3527. https://doi.org/10.1016/J.BIORTECH.2007.07.052.

Poreba, R., Gac, P., Poreba, M., Derkacz, A., Pilecki, W., Antonowicz-Juchniewicz, J., Andrzejak, R., 2010. Relationship between chronic exposure to lead, cadmium and manganese, blood pressure values and incidence of arterial hypertension. Med. Pr. 61 (1), 5–14.

Rhazi, L., Lakahal, L., Andrieux, O., Niamba, N., Depeint, F., Guillemet, D., 2020. Relationship between the molecular

characteristics of Acacia gum and its functional properties. Food Chem. 126860. https://doi.org/10.1016/j.foodchem.2020.126860.

Sene, C., McCann, M.C., Wilson, R.H., Grinter, R., 1994. Fourier-transform Raman and Fourier-transform infrared spectroscopy (an investigation of five higher plant cell walls and their components). Plant Physiol. 106, 1623–1631. https://doi.org/10.1104/pp.106.4.1623.

Sharma, A., Bhattacharyya, K.G., 2005. Adsorption of Chromium (VI) on Azadirachta Indica (Neem) Leaf Powder. Adsorption 10, 327–338. https://doi.org/10.1007/s10450-005-4818-x.

Showalter, A.M., 2001. Arabinogalactan-proteins: structure, expression and function. CMLS. Cell. Mol. Life Sci. 58, 1399–1417. https://doi.org/10.1007/PL00000784.

Siddig, N.E., Osman, M.E., Al-Assaf, S., Phillips, G.E., Williams, P. A., 2005. Studies on acacia exudate gums, part IV. Distribution of molecular components in Acacia seyal in relation to Acacia senegal. Food Hydrocoll. 19 (4), 679–686. https://doi.org/10.1016/j.foodhyd.2004.09.005.

Smith, B.C., 2017. An IR spectral interpretation potpourri: Carbohydrates and Alkynes. Spectrosc. 32(7), 18-24. [WWW Document]. URL http://www.spectroscopyonline.com/ir-spectral-interpretation-potpourri-carbohydrates-and-alkynes (accessed 4.28.20).

Smith, R.M., Motekaitis, R.J., Martell, A.E., 1985. Prediction of stability constants. II. Metal chelates of natural alkyl amino acids and their synthetic analogs. Inorg. Chim. Acta 103, 73–82. https://doi.org/10.1016/S0020-1693(00)85215-9.

Soco, E., Kalembkiewicz, J., 2016. Comparison of adsorption of Cd (II) and Pb(II) ions on pure and chemically modified fly ashes. Chem. Process Eng. 37.

Song, C., Wu, S., Cheng, M., Tao, P., Shao, M., Gao, G., 2014. Adsorption studies of coconut shell carbons prepared by KOH activation for removal of lead(II) from aqueous solutions. Sustainability. 6 (1), 86–98. https://doi.org/10.3390/su6010086.

Su, P., Granholm, K., Pranovich, A., Harju, L., Holmbom, B., Ivaska, A., 2012. Metal ion sorption to birch and spruce wood. BioResources 7, 2141–2155.

Subbaiah, M.V., Yuvaraja, G., Vijaya, Y., Krishnaiah, A., 2011. Equilibrium, kinetic and thermodynamic studies on biosorption of Pb(II) and Cd(II) from aqueous solution by fungus (Trametes versicolor) biomass. J. Taiwan Inst. Chem. Eng. 42, 965–971. https://doi.org/10.1016/j.jtice.2011.04.007.

Synytsya, A., Čopíková, J., Matějka, P., Machovič, V., 2003. Fourier transform Raman and infrared spectroscopy of pectins. Carbohydrate Polym. 54, 97–106. https://doi.org/10.1016/S0144-8617(03)00158-9.

Tan, L., Showalter, A.M., Egelund, J., Hernandez-Sanchez, A., Doblin, M.S., Bacic, A., 2012. Arabinogalactan-proteins and the research challenges for these enigmatic plant cell surface proteoglycans. Front. Plant Sci. 3, 140. https://doi.org/10.3389/fpls.2012.00140.

Temkin, M.I., 1940. Kinetics of ammonia synthesis on promoted iron catalysts. Acta Physiochim. URSS 12, 327–356.

Togue Kamga, F., 2018. Modeling adsorption mechanism of paraquat onto Ayous (Triplochiton scleroxylon) wood sawdust. Appl. Water Sci. 9, 1. https://doi.org/10.1007/s13201-018-0879-3.

Vilar, V.J.P., Botelho, C.M.S., Boaventura, R.A.R., 2007. Kinetics and equilibrium modelling of lead uptake by algae Gelidium and algal waste from agar extraction industry. J. Hazard. Mater. 143, 396–408. https://doi.org/10.1016/j.jhazmat.2006.09.046.

Wang, S., Hung, C., 2003. Electromagnetic shielding efficiency of the electric field of charcoal from six wood species. J. Wood Sci. 49, 450–454 (2003). https://doi.org/10.1007/s10086-002-0506-6.

Wani, A.L., Ara, A., Usmani, J.A., 2015. Lead toxicity: a review. Interdiscip. Toxicol. 8 (2), 55–64. https://doi.org/10.1515/intox-2015-0009.

Waseem, S., Din, M.I., Nasir, S., Rasool, A., 2014. Evaluation of acacia nilotica as a non conventional low cost biosorbent for the elimination of PB(II) and CD(II) ions from aqueous solutions. Arab. J. Chem. 7 (6), 1091–1098. https://doi.org/10.1016/J.ARABJC.2012.03.020.

Weber, T.W., Chakravorti, R.K., 1974. Pore and solid diffusion models for fixed-bed adsorbers. AIChE J. 20, 228–238. https://doi.org/10.1002/aic.690200204.

Yang, X., You, F., Zhao, Y., Bai, Y., Shao, L., 2018. Tunneling-induced negative permittivity in Ni/MnO nanocomposites by a biogel derived strategy. ES Energy Environ. 1, 106–113. https://doi.org/10.30919/esee8c142.

Zabochnicka-Świątek, M., Krzywonos, M., 2014. Potentials of Biosorption and Bioaccumulation Processes for Heavy Metal Removal. Pol. J. Environ. Stud. 23 (2), 551–561.

Zafar, M.N., Nadeem, R., Hanif, M.A., 2007. Biosorption of nickel from protonated rice bran. J. Hazard. Mater. 143, 478–485.